~~250 years~~ A 258-year-long data set of ~~daily weather: Temperature~~ temperature and precipitation fields for Switzerland since 1763

Noemi Imfeld[1,2], Lucas Pfister[1,2], Yuri Brugnara[1,2], and Stefan Brönnimann[1,2]

[1]Oeschger Center for Climate Change Research, University of Bern, Switzerland
[2]Institute of Geography, University of Bern, Switzerland

Correspondence: Noemi Imfeld (noemi.imfeld@giub.unibe.ch)

Abstract. Climate reconstructions give insights in monthly and seasonal climate variability of the past few hundred years. However, for understanding past extreme weather events and for relating them to impacts, for example through crop yield simulations or hydrological modelling, reconstructions on a weather time scale are needed. Here, we present a data set of ~~250~~ 258 years of daily temperature and precipitation fields for Switzerland for 1763 to 2020. The data set was reconstructed with the analogue resampling method which resamples meteorological fields for a historical period based on the most similar day in a reference period. These fields are subsequently improved with data assimilation for temperature and bias correction for precipitation. Even for an early period prior to 1800 with scarce data availability, we found good validation results for the temperature reconstruction especially in the Swiss Plateau. For the precipitation reconstruction, skills are considerably lower, which can be related to the few precipitation measurements available and the heterogeneous nature of precipitation. By means of a case study on the wet and cold years from 1769 to 1772, which triggered wide-spread famine across Europe, we show that this dataset allows more detailed analyses than hitherto possible.

1 Introduction

Reconstructions of atmospheric variables on monthly, seasonal, and annual time scales have allowed for studying climate variability of the past few hundred years and helped to gain relevant insights into long-term changes and variability (e.g. Luterbacher et al., 2004; Casty et al., 2005, 2007; Dobrovolnỳ et al., 2010; Murphy et al., 2020; Valler et al., 2022). However, for various applications, such as assessing climate impacts, rather than the monthly or seasonal variability, daily weather is more relevant (Brönnimann, 2022). Temperature and precipitation fields on a daily time scale for past extreme events allow us to conduct impact modelling for example of crop yields (Flückiger et al., 2017), phenological stages of specific species (Rutishauser et al., 2020), runoff (Rössler and Brönnimann, 2018), and avalanche disposition (Brugnara et al., 2017; Pfister et al., 2020). Numerous historical sources report on past extreme weather events with severe impacts on society (e.g., Pfister and Wanner, 2021) that could be better understood using daily weather fields. One example that will be followed up in this article are the wet-and-cold anomalies in the late 18th century in Europe that led to wide-spread famine (Collet, 2018).

In Europe, efforts have been undertaken to reconstruct meteorological fields dating back to the 19th century. For example, Devers et al. (2021) created a high-resolution reanalysis covering France for the period 1870 to 2012. They assimilated daily

temperature and precipitation observations into the SCOPE climate reconstruction (Caillouet et al., 2019) using an offline Ensemble Kalman Filter. When sufficient data are available, fields can be reconstructed based on interpolation methods such as for the UK for daily precipitation fields dating back to 1890 (Keller et al., 2015). Single weather events have been reconstructed by resampling present-day meteorological fields (Pappert et al., 2022; Flückiger et al., 2017) and by dynamically downscaling historical reanalysis data (e.g., Stucki et al., 2015; Brugnara et al., 2017). Both reconstruction methods yielded insights into the evolution and spatial extent of these past weather and climate events. Also, the use of documentary sources from weather diaries has been explored for reconstructing past weather with different approaches (Harvey-Fishenden and Macdonald, 2021; Wang et al., 2021). For Switzerland, Pfister et al. (2020) reconstructed daily temperature and precipitation fields for 1864 to 2017 based on the analogue resampling method (ARM). This method resamples meteorological fields for a historical period based on the most similar day in a reference period. Subsequently, temperature measurements were assimilated onto the temperature fields and a quantile mapping was applied to correct for biases in the precipitation fields. Both variables showed a very good reconstruction performance as illustrated by a case study on the avalanche winter 1887/88 (Pfister et al., 2020). The analogue method has been widely used in climate and weather reconstruction (e.g. Schenk and Zorita, 2012; Gómez-Navarro et al., 2017) with considerable skill.

Weather recording peaked for the first time as early as around the late 18th century (Brönnimann et al., 2019). However, only a few attempts have been made to reconstruct weather back to this time using quantitative data (e.g., Pappert et al., 2022). For this period, only a few data records have so far been available, because it is tremendous work to find, image, digitize, quality check, and homogenize these data. For Switzerland, recent data rescue projects made available a unique set of historical instrumental data before 1864, the so-called early instrumental data (Brugnara et al., 2020b; Pfister et al., 2019). This data makes it possible to reconstruct temperature and precipitation fields for Switzerland back to the mid-18th century.

Here, we present a new data set of daily temperature and precipitation fields for Switzerland with higher resolution spanning the last 250 258 years. It consists of two subsets: (1) a new reconstruction from 1763 to 1863 described in this article and (2) an update of the reconstruction by Pfister et al. (2020) with a higher resolution of 1 km and spanning 1864 to 2020. Reconstructions were made with the analogue resampling method and subsequent data assimilation for temperature and bias correction for precipitation. This data set allows further applications to other fields, such as environmental impact studies and crop yield modelling.

During the years 1769 to 1772, Europe suffered from one of the most severe famines of the little ice age (Collet, 2018; Pfister and Brázdil, 2006), which has been related to a cultural crisis and a climatic wet-cold anomaly. We use this event to exemplary calculate climate indices that had an impact on crop growth in Switzerland and to compare it to documentary data describing the event (Collet, 2018; Pfister and Brázdil, 2006).

The paper is structured as follows. The second section Section two describes the data needed for the reconstruction, and the third section . Section three describes the reconstruction method and how we evaluate the reconstruction skill. Section four shows and discusses these evaluation results and in section five we showcase the use of the reconstruction based on a case study. The conclusion is found in section six. The data set is available online at Pangaea (link not yet availablehttps://doi.pangaea.de/10.1594/PANGAEA.950236) (Imfeld, 2022).

2 Data

2.1 Historical instrumental data

Systematic measurements of meteorological data in Switzerland only started in the 1860s with the establishment of the national weather service (Hupfer, 2019; Begert et al., 2005). To reconstruct weather in the late 18th and early 19th century we, therefore, relied on data that has been rescued in various initiatives (Brugnara et al., 2020b; Pfister et al., 2019; Camuffo and Jones, 2002; Klein Tank et al., 2002; Füllemann et al., 2011; Brugnara et al., 2022). Such early instrumental data are challenging to work with because common measurement standards had not yet been developed when the observations were recorded. ~~Common difficulties~~ Difficulties with early instrumental data arise for example from the construction of the ancient measurement devices, unknown measurement devices ~~or~~ and liquids, inappropriate location of the devices, exposure to radiation, and missing or ambiguous observation times (Brugnara et al., 2020b). For early temperature measurements, for example, unstable glasses contracting with age, differences in the expansion rate of the liquids in the glass, and exposure to radiation or precipitation can create errors in the measurements (Brugnara et al., 2020b; Winkler, 2006; Böhm et al., 2010). It was already recognized in the 18th century that a thermometer needs to be sheltered from solar radiation (Pfister, 1988). However, even thermometers placed on north-facing walls, as was common after 1760, were still influenced by radiation (Böhm et al., 2010) and often showed warm biases. Sources of errors for pressure measurements include device-related issues (Brugnara et al., 2020a), but also the required temperature corrections due to the thermal expansion of the liquid in the barometers. Temperature corrections can introduce errors in pressure measurements, when no attached thermometer is available, when temperature measurements are not representative ~~for~~ of the barometer, or when applied corrections are unclear.

The manual measurements in our network were taken between two to eight times per day. Calculating an arithmetic daily mean for temperature and pressure based on only a few measurements a day or on varying measurement times introduces biases in daily means. Also, ~~a common problem with~~ observation times of early instrumental data ~~are ambiguousobservation times, such~~ can be ambiguous, for example when the time is denoted as "morning" or "evening" and ~~how~~ it is therefore not straightforward to include these in a daily mean estimation. These above-described examples affect the quality of measurements used for the reconstruction and corrections are often difficult. The quality of early instrumental data thus has to be kept in mind, when working with the reconstruction.

For the reconstruction from 1763 to 1863, we selected time series that showed sufficient data quality (Brönnimann, 2020) and that cover at least seven continuous years to keep the reconstruction as spatially and temporally consistent as possible and time series ~~that showed sufficient data quality (Brönnimann, 2020)~~. However, the network changes considerably throughout time (Fig. 1) and coverage is much scarcer compared to the network after 1864, which has been used for the reconstruction from 1864 to 2020 in Pfister et al. (2020) (Fig. 1d and e). At the start of the reconstruction period in 1763, around 11 to 12 series are available (Fig. 1a) which then increases to around 30 series (Fig. 1c). To increase the number of observations for this early period we also used time series from nearby locations in Italy and Germany. In total, the reconstruction is based on 17 pressure series, 18 temperature series, and 6 precipitation and precipitation occurrence series. Because only very few precipitation measurements were available, we also include precipitation occurrence as a variable, that has been derived from weather notes.

Figure 1f shows the evolution of monthly data availability and Table 1 lists all time series used in the reconstruction period 1763 to 1863.

Most of the instrumental data for the reconstruction were already available in modern units and its quality was checked on a subdaily basis (for details see Brugnara et al., 2020b). The data preparation necessary included thus the calculation of daily mean values, pressure reduction where not available, additional quality control on daily means, and the homogenization of the time series.

To adjust the daily mean value based on only a few subdaily measurements, we subtracted a correction according to the historical measurement times. These corrections were calculated for every month of the year separately based on the anomalies of the 10 minutes monthly means from automatic weather stations for the period 1981 to 2010. If no weather stations were available in the surrounding area, the corrections were calculated from the hourly 2-meter temperature of the closest grid point from ERA5-Land (Muñoz-Sabater et al., 2021) for 1981 to 2010. The anomalies were calculated by subtracting the daily mean of each month from the ~~10 minute~~ 10-minute measurements. The final correction value was obtained by taking the mean of the anomalies according to the closest measurement times. For pressure, the daily mean correction was applied for all time series using the closest grid point from hourly ERA5-Land surface pressure data for 1981 to 2010. If no observation times were available, we tried to estimate the observation times by comparing the subdaily values to the daily cycle derived from present-day measurements, which however can introduce additional errors. For three time series, a temperature reduction of pressure has not been conducted because no attached temperature measurements have been found. Therefore, we reduced the pressure to $0°$ C based on the climatology of daily mean temperature data for the period 1850 to 1900 from the reanalysis 20CRv3 (Slivinski et al., 2019; Brugnara et al., 2020b). For subdaily weather notes, every day containing at least one precipitation event was transformed into a precipitation day. We did not convert descriptions such as dew and rime to precipitation, because it was not available for all stations.

Further, we performed a standard quality control on the daily means of each time series as it is implemented in Brugnara et al. (2019) and a spatial quality control using linear regression between the nearby five stations (Estévez et al., 2018). Together with the standard quality control, we flagged between 0 to 1.16 % of the values (with a mean of 0.12 %) depending on the time series. For precipitation occurrence, we calculated monthly wet day frequency for the series and excluded series that substantially deviated from other series or that showed substantial visual breaks.

We homogenized the quality controlled series using surface temperature, respectively pressure from the closest grid point of the EKF400v2 reanalysis (Valler et al., 2022) as a reference series (see Sect. 2.4). Break point detection was performed with the penalized maximal t-test (Wang et al., 2007) and the penalized maximal F-test (Wang, 2008), which are implemented in Wang and Feng (2013). Only break points that were significant without metadata were considered ~~,~~ since only very few metadata are available. For Bern, Zurich, Basel, and Geneva homogenized series were used, ~~that~~ which are based on various short series (Brugnara et al., 2022; Brugnara, 2022).

As an independent evaluation of our reconstruction, we used seven temperature time series and one time series of precipitation occurrence during 1763 and 1863 (see asterisks in Fig. 1a and Table 2). The temperature time series were prepared follow-
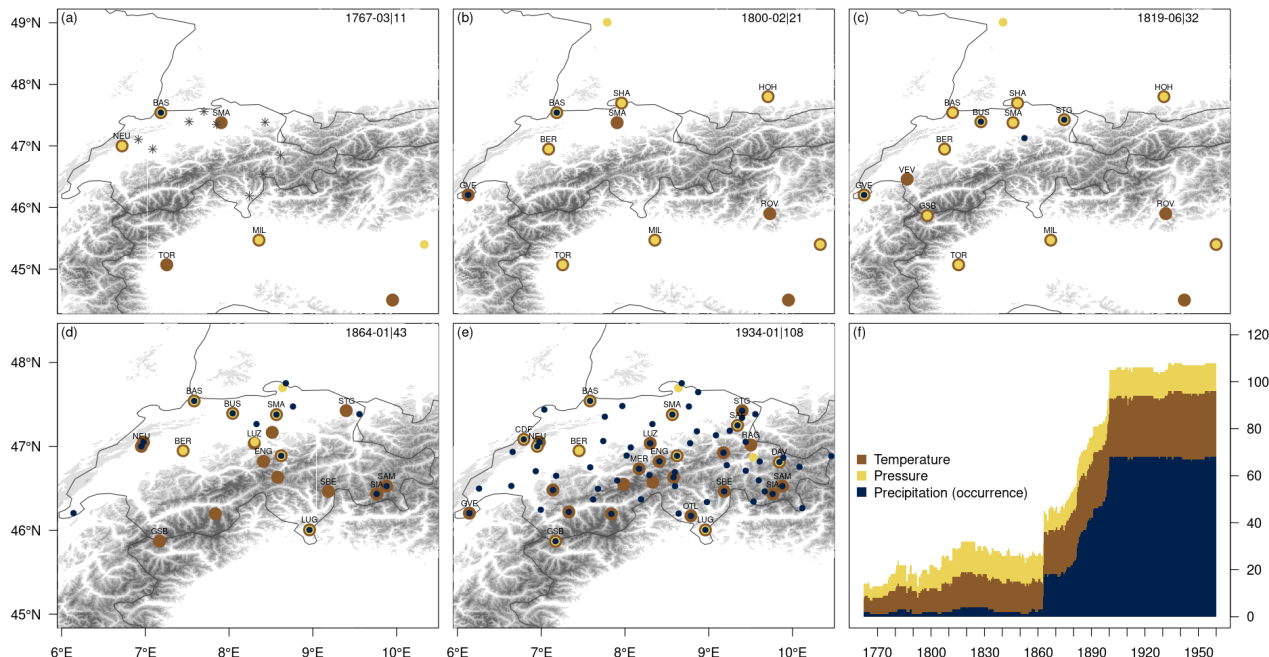
Figure 1. a-e) Station measurements as they are available for five different months ~~during~~ from 1763 to 1960. The upper right numbers denote the example month and the total number of measurements for this time ~~steps~~step. ~~Stations with a name~~ Labeled stations are used in the ensemble Kalman ~~Fitting~~fitting. d and e) show the networks as ~~they are~~ used in Pfister et al. (2020). Asterisks in (a) denote locations of independent measurements, which are used for an evaluation of the reconstruction. f) Evolution of temperature, pressure, and precipitation measurements throughout the entire period. Precipitation includes precipitation occurrence and precipitation measurements.

ing the same approach as for the series used in the reconstruction itself, but ~~we did not homogenize them~~no homogenization was performed.

2.2 Present-day instrumental data

The analogue selection requires for every historical time series an equivalent series in the reference period from 1961 to 2020. The long historical time series in Switzerland are mainly found in large cities. These locations also have a measurement station in the Swiss National Basic Climate Network (NBCN) (Füllemann et al., 2011; Begert et al., 2007). Precipitation and temperature time series from this network are quality controlled and homogenized by the Swiss Meteorological Service (Begert et al., 2005). For locations in Switzerland, where no data from the NBCN is available, we extracted the closest grid point from the daily temperature and precipitation fields (TabsD and RhiresD, for details about data sets, see next section), and for sea level pressure from the European EOBS data set v23.1 (Cornes et al., 2018). For time series in Germany and Italy, we used daily ECA&D station data (Klein Tank et al., 2002) if available or as well the closest grid points from EOBS. To create time series of precipitation occurrence in the reference period, we used ~~a threshold of >~~for each series individual thresholds between

5

140 0.1 and 1 mm for a rainy day. This is needed since the historical time series differ in how a wet day has been written down. To be able to use the full reference period as an analogue pool, all series in the reference period were gap filled by applying a quantile mapping between the gridded data set (mainly EOBS) and the ~~non missing~~ non-missing data of the time series. This bias correction is needed because a grid cell does not capture the local characteristics of a station, and may thus have systematic biases. We choose an empirical quantile mapping that estimates empirical cumulative distribution functions for the grid cell

145 and station time series for 99 percentiles with a linear interpolation between the percentiles (Gudmundsson et al., 2012). The quantile mapping was calculated for every day of the year individually including +/- 15 days around the target day because the biases between the grid and stations showed an annual cycle. The same approach was used to extend the station data up to 2020 or back to 1961 ~~,~~ if they did not cover the full period from 1961 to 2020. Further, if it was not yet done, we homogenized the series with the closest homogenized NBCN stations as a reference using the penalized maximal t-test (Wang et al., 2007)

150 and the penalized maximal F-test (Wang, 2008) as implemented in Wang and Feng (2013) for break point detection. Table 1 summarizes the information on the reference stations.

2.3 Gridded data sets

The analogue fields are resampled from the two daily spatial data sets from MeteoSwiss for temperature (TabsD) and precipitation (RhiresD) (MeteoSwiss, 2021b, a). These data sets are available for the period from 1st January 1961 to 31st December

155 2020 at a resolution of 1x1 km. The temperature fields represent the free-air temperature at two meters above ground and are interpolated from approximately 90 homogeneous long-term station series with a deterministic analysis method using non-linear vertical temperature profiles and non-Euclidean distance (Frei, 2014). The precipitation fields cover all hydrological catchments that drain to locations within the Swiss border (MeteoSwiss, 2021a), i.e. also areas outside Switzerland. For the reconstruction, we only use the area that is covered during the entire 60 years excluding catchments to the south of Valais.

160 The precipitation fields are generated using around 650 rain-gauge measurements within Switzerland and from neighbouring countries. They are based on spatially interpolated monthly mean precipitation of a day and spatial interpolations of relative anomalies (MeteoSwiss, 2021a).

2.4 Additional data sets

We want to restrict the selection of analogue days to days of similar weather. Therefore, we used a reconstruction of daily

165 weather types covering the period 1763 to 2009 from Schwander et al. (2017). This reconstruction is based on instrumental station records across Europe and the weather type classification by Weusthoff (2011). The weather type reconstruction also contains probabilities of the weather types for each day to account for the uncertainty of the reconstruction. For the period after 2009, we used the weather types provided by MeteoSwiss (Weusthoff, 2011).

The pre-processing steps of the gridded fields and observational data require additional reanalysis data. We use the palaeo-

170 reanalysis EKF400v2 (Valler et al., 2022) for homogenization of station data and for calculating a climatic offset between the reference period and the historical period to account for the warming since the pre-industrial period. This palaeo-reanalysis is based on atmosphere-only general circulation model simulations and assimilates a variety of data, such as early instrumental

6

temperature and pressure data, documentary data, and tree-ring records. The reanalysis ERA5 (Hersbach et al., 2020) was used to remove temperature trends in the reference period (see Sect. 3.1).

175   In addition, we use the two monthly reconstructed gridded data sets for Switzerland TrecabsM1864 and RrecabsM1864 covering the period 1864 to 2020, which have been constructed with a focus on high temporal consistency (MeteoSwiss, 2021c).

3   Method

For the analogue reconstruction, we mainly followed the approach implemented in Pfister et al. (2020). Some adaptations were

180   necessary to reconstruct the early period from 1763 to 1863, because of the different network densities, and different data types, and because the data set extended further back in time. This adapted approach is described in the following sections. The period 1864 to 1960 was reconstructed as in Pfister et al. (2020) with the exception that we removed the trend in the temperature data of the reference period (see Sect. 3.1), we changed the error covariance calculation of the observations for the assimilation procedure (see Sect. 3.3), and we implemented a quantile mapping approach considering the annual cycle of the precipitation

185   bias (see Sect. 3.4). Figure 2 shows all required steps for creating the final reconstruction, including the data preparation, the reconstruction, and the cross-validation.

3.1   Pre-processing

Before the analogue selection, the observations had to be pre-processed to make the historical observations comparable to the observations in the reference period from 1961 to 2020. Firstly, we removed the trend for the temperature data (observations

190   and grids) in the reference period to make it equally likely to choose as analogues, days from warmer years of the 21st century. To remove a trend representing average climatic changes (and not local climatic changes), we calculated a linear trend for the 2 meter temperatures from the zonal mean of the ERA5 reanalysis covering the period 1961 to 2020 centered at 1991. For each grid cell and station, the trend of the closest latitude was subtracted. Secondly, for the analogue selection and for the resampling in the historical period before the year 1864, we removed a climatic offset from the reference temperature observations and the

195   grid, because the temperature data are warmer in the reference period than in the historical period 1763 to 1863. A monthly transient offset was calculated based on the difference between the zonal mean temperature of a 31-years 31-year window centered around the reconstructed year (e.g. from 1748 to 1778 for the year 1763) and the zonal mean temperature in the reference period 1961 to 2003 considering land areas only. In this case, the reference period is shorter, because the EKF400v2 reanalysis ends in 2003. This offset was then subtracted from the data in the reference period (grid and observation) for every

200   reconstructed day. Further, the historical stations had to be homogeneous with respect to their reference station. We performed a simple homogenization by calculating monthly differences between the historical and reference station over the full available period with respect to the closest grid points of the respective variable from the reanalysis EKF400v2 (Valler et al., 2022). The resulting difference of these two series is subtracted from the historical series to adjust them towards EKF400v2. Lastly, we
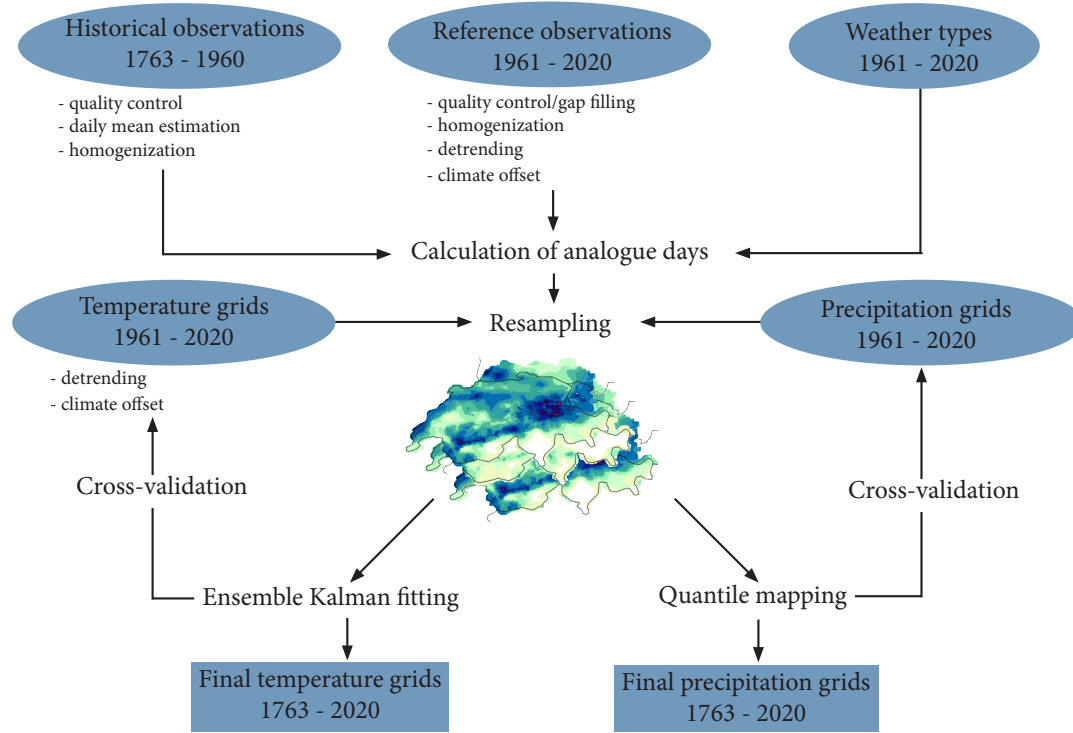
Figure 2. Schematic of temperature and precipitation reconstruction. Blue ellipses show input data. The necessary data preparation steps are listed below the input data. Blue rectangles show the final output data. Details on the individual steps are found in Chapter 3.

removed the seasonal cycle of temperature by fitting the first two harmonics of the temperature time series for observations

205   and grid cells using least squares (see Pfister et al. (2020) for the equation).

3.2   Analogue reconstruction

The ARM samples meteorological fields for a historical period from the most similar days in a reference period. The most similar days, called the analogue days, are the days with the smallest distances calculated between the observational data in the historical period and observational data in the reference period. Our historical period starts in 1763 and is limited at the lower

210   end by the availability of reconstructed weather types (Schwander et al., 2017). The reference period covers the period of the two gridded data sets TabsD and RhiresD from 1961 to 2020. These gridded data are resampled to generate a first reconstruction based on the best analogue day. To ensure that only physically plausible analogue days were chosen, the analogue selection

was constrained to days with a similar weather type and days within the same season. All weather types with a cumulative probability of 95 % for the target days were admitted to the analogue pool to account for the uncertainty in the weather type reconstruction. This means ~~,~~ we added up the probabilities of the most likely weather types until they reached together 95 %. Weather type probabilities were lower for the early days of the reconstruction in the 18th and beginning of the 19th century. For individual days, probabilities were so low (e.g. for 1803-03-01), that all weather types were included in the analogue pool. But the days of the analogue pool were still constrained by the seasons. A season was defined based on a moving window of +/- 60 days centered ~~at~~ on the target day.

To reconstruct fields before 1864, we also used daily weather notes transformed ~~to~~ into binary values of precipitation occurrence. The distance metrics used to find the closest analogue days in Pfister et al. (2020), the root mean squared error (RMSE), can however not be applied to categorical data (i.e. precipitation occurrence). Instead, we used the Gower distance, ~~that~~ which allows for distances to be calculated for different variable types, such as continuous and count data (Gower, 1971; Kuhn and Johnson, 2019). It is defined as the average of partial distances across the variables (Eq. 1):

$$d(ij) = \frac{1}{k} \sum_{k=1}^{k} d(i,j,k) \tag{1}$$

The partial distances are calculated as a range-normalized Manhattan distance for the quantitative variables temperature, pressure, and precipitation sum. For the binary variable precipitation occurrence, the partial distances are calculated as follows. If $x_i k = x_j k$, then the partial distance ~~of~~ is $d_i jk = 0$, and otherwise if $x_i k$ is not equal to $x_j k$, $d_i jk = 1$. We used an unweighted Gower distance. Thus, the distance metric for precipitation occurrence was either minimal (0) or maximal (1) which increased the weight of precipitation occurrence in the selection of the closest analogue. A first reconstruction was then obtained by resampling the fields based on the analogue day with the closest distance. For updating the newer period from 1864 to 1960 we used the RMSE as a distance measure because a lot more precipitation measurements were available (compared to the earlier period) and the RMSE penalizes large errors. Changing the distance measure within the reconstruction period could lead to inhomogeneities. However, evaluations with both measures showed that the differences between the measures are small and the differences caused by the network changes are much larger.

3.3 Data assimilation for temperature fields

In a next step, the resampled temperature fields were improved by assimilating the available temperature measurements using ensemble Kalman fitting. This is an offline data assimilation approach, where the analysis is not passed to the next time step, i.e. every time step is handled individually (Bhend et al., 2012; Valler et al., 2022). Data assimilation tries to find an optimal representation of the true atmospheric state between the best guess of an atmospheric field (our best analogue field) and the observations by minimizing a cost function (Franke et al., 2017). In the case of normally distributed errors, this cost function can be minimized with a Kalman filter. The best estimate of a true atmospheric state, the analysis x^a, is given by Eq. (2):

$$x^a = x^b + P^b H^T (H P^b H^T + R)^{-1} (y - H x^b) \tag{2}$$

where x^b refers to the best estimate (the resampled analogue fields), P^b is the model error covariance matrix calculated from the 50 best analogues for each target day, H extracts the observations from the model space, and R is the observation error covariance matrix. The second part on the right-hand side of the Eq. (2) $P^b H^T (H P^b H^T + R)$ is referred to as the Kalman gain K. To account for a bias in the covariance analysis, we used the ensemble square root filter as proposed by Whitaker and Hamill (2002) and updated the ensemble mean and the anomaly from the ensemble mean individually yielding to separate equations Eq. (3) and (4).

$$\bar{x}^a = \bar{x}^b + K(\bar{y} - H\bar{x}^b) \tag{3}$$

$$x'^a = x'^b + \tilde{K}(y' - Hx'^b) \quad \text{with: } y' = 0 \tag{4}$$

The Kalman gain for the mean K and anomaly $\tilde{K}$ were then calculated as follows.

$$K = P^b H^T (H P^b H^T + R)^{-1} \tag{5}$$

$$\tilde{K} = P^b H^T ((\sqrt{H P^b H^T + R}^{-1})^T \times (\sqrt{H P^b H^T + R} + \sqrt{R})^{-1} \tag{6}$$

Often a localization of the background error covariance matrix P^b is used in data assimilation to avoid spurious error covariance. Testing different distance-, altitude-, and correlation-adjusted localization as proposed by Devers et al. (2021) did not improve results in our rather small area. Therefore, we did not apply a localization.

We estimated the observation error covariance assuming that there is a linear relationship with distance between the variance of the differences in neighbouring observations as proposed by Wartenburger et al. (2013). The error covariance was estimated for the three periods 1763 to 1863, 1864 to 1960, and 1961 to 2020 individually. As to be expected, errors in the last period 1961 to 2020 were smaller and thus the skill of the cross-validation was overestimated. Due to the few available measurements within Switzerland in the period 1763 to 1863, we assimilated also the temperature data from Hohenpeissenberg, Torino, Milano, and Rovereto. To do this, the observations from the best analogue days of the stations outside of Switzerland (and therefore outside of our grid) were added to the background x^b, and subsequently, the H operator was adjusted and P^b was calculated including these observations. The observation errors for these stations outside of Switzerland were calculated as described above. For the years after 1864, only stations with correlation values above 0.975 are used for assimilation (see named stations Fig. 1d and e). Before assimilating the observations we removed a monthly bias calculated between the observation and the closest grid points from the observations , because the observations are biased with respect to the model grid.

3.4 Quantile mapping for precipitation fields

Despite using the same grids, precipitation biases occurred in the analogue based reconstruction because precipitation measurements are very scarce and unevenly distributed across the area, leading to systematic biases in areas with no precipitation observations. To correct for these biases, we apply an empirical quantile mapping calibrated between the reconstruction in the

reference period and the original data set (RhiresD) for every grid cell (Gudmundsson et al., 2012; Feigenwinter et al., 2018; Rajczak et al., 2016). Correction factors were estimated for the 1st to 99th percentile using a linear interpolation between the percentiles. A wet-day threshold was set to 0.1 mm. Because the quantile mapping showed seasonal biases of up to 1 mm per day in southern Switzerland when the quantile mapping was estimated for the entire year, we calculated it in ~~five day~~ fifteen days steps throughout the year based on a 91-days window centered around these ~~five~~ fifteen days. This yielded a total of ~~73~~ 24 steps, which was a compromise between doing a bias correction for every day of the year individually, and doing the bias correction only for the four seasons. Because the biases in the precipitation reconstruction changed considerably based on the station network, the quantile mapping was computed for the different networks (see Fig. 1) and then applied to the historical reconstruction depending on what network the historical period corresponded best. Note that Fig. 1 only shows three examples of networks for the period before 1864. The quantile mapping was conducted for six different set-ups based on the most often occurring station combinations.

3.5 Evaluation

To ~~test the reconstruction skills~~ evaluate the skill of the reconstructions, we performed (1) a cross-validation in the reference period 1961 to 2020 and (2) compared the reconstructed fields with time series in the early period that have not been used for the reconstruction. For the cross-validation, we reconstructed the temperature and precipitation fields for the reference period 1961 to 2020. For every day, the best analogue days were calculated by leaving out -/+ five days around the target day. The reconstructed fields were then compared to the original fields using five standard measures. We calculated the root mean squared error (RMSE), Pearson correlation, mean bias, and the mean squared error skill score (MSESS) on the deseasonalized temperature anomalies. For the MSESS, we used climatology as a reference, which is zero in the case of anomalies. For precipitation we used the Spearman correlation, RMSE, mean bias, and the Brier score (Wilks, 2011). We used the Brier score to evaluate how well the reconstruction assigns wet and dry days. Therefore instead of probabilities the Brier score was calculated for wet and dry days using 0.1 mm as a threshold. The Brier score returns the percentage of days that are wrongly assigned as wet or dry days. To assess the temporal persistence of the reconstruction on the day-to-day timescales in more detail, we performed two additional analyses. For temperature, we calculated the autocorrelation at a 1-20 days lag for all networks and compared these values to the autocorrelation in the original grid TabsD. For precipitation, we used two persistence indices suggested by Moon et al. (2019) to assess the mean persistence characteristics of precipitation and compared these to the persistence calculated with the original RhiresD grid.

   Because the station network changes heavily over time, we performed the cross-validation for the different network set-ups shown in Fig. 1. ~~This~~ The evaluation is done for every grid cell independently, i.e. evaluating the reconstruction in time. For the network shown in Fig.1c, we also compared the original and reconstructed grids area-wise by calculating the above mentioned measures in space and for two different altitude levels from 0 to 1000 msl and from 1000 to 2000 msl for an area in Central Switzerland between 7.4 to 9.1° E and 46.5 to 47.3° N. This gives insights, how well the spatial structure is reproduced. The final reconstruction is, however, run on all available data.

~~Furthermore, we evaluated~~ For an independent evaluation, we compare the reconstruction with station data from seven entirely independent temperature series in the period 1763 to 1863 (see Table 2) based on the same measures as described above. The mean bias was not calculated for series with removed seasonality, but for the absolute temperature series. The precipitation reconstruction was compared at the location of Bern to an independent series based on the Brier score and by comparing monthly wet-day frequencies of the observation and the closest grid cell of the reconstruction. Furthermore, we explore the representation of the long-term variability by comparing our reconstructions to other datasets covering the same or similar periods.

4 Results and Discussion

4.1 Cross-validation during reference period

Cross-validation results for deseasonalized temperature anomalies using the network as in Fig. 1c (i.e. a dense network for the historical period) shows correlation values between 0.67 to 0.99 and an average of 0.92 to 0.95 (Fig. 3a to e) for all seasons and the annual evaluation. All periods show a spatial pattern with the highest correlations in the Swiss Plateau, lower values in the Alpine region, and lowest ~~values~~ in the canton of Ticino. The winter months (December to February) show the lowest correlation values, especially in the Alpine region, followed by autumn (SON) and spring (MAM). These spatial and seasonal differences are also present in the RMSE and MSESS evaluation (Fig. 3f to o). RMSEs range between 0.45 to 3.82° C, with an average of 1.04 to 1.59° C for all time aggregations. In winter, the errors are largest in the very south and east of Switzerland, and in the Jura. MSESS values range between 0.34 and 0.98. The lowest values are found in the valleys of Ticino, especially around the Lago Maggiore in winter and autumn. Mean biases range between -0.34 and +0.08° C (Fig. 3p to t). In winter, pronounced cold biases are present in the Alpine region, southern Switzerland, and the Jura. This is also the case for autumn, but biases are smaller. In spring, largest cold biases are mainly found in the Alps, but not Ticino, whereas in summer, biases range only between -0.06 to +0.08° C.

Spatial correlations do not show large differences in their performance with respect to the different deciles of the area mean for summer and winter and both altitude groups (Fig.4a and b). In winter, RMSEs are larger for the coldest and the warmest days while days in the middle of the distribution show lower errors. Especially at altitudes above 1000 msl, the warmest days show larger RMSEs. In summer, cold days have low RMSEs, and the RMSEs increase with increasing temperatures. This effect is more pronounced for the higher altitude group. The mean bias in the low altitude group (below 1000 msl) does not show differences in the deciles. However, for the higher altitude group, the very cold days are too warm in the reconstruction and the very warm days are too cold. In summer, such an effect is not visible, but the spread of the mean bias distribution is generally larger for ~~the~~ warm days than ~~the~~ cold days.

Cross-validation results of the different networks, however, vary considerably. The network with only 11 measurements (Fig. 1a), has the lowest correlations ~~values and they range~~ with values ranging between 0.58 to 0.99 for winter and 0.64 to 0.99 for summer (Fig. 5a and b). Especially in the winter months, this network performed worse with respect to correlation, RMSE, and MSESS. In summer, differences between networks ~~were~~ are much smaller (Fig. 5b). The increase in observations in 1864

showed for all metrics much better performance, however, the change in the network from 41 observations to 108 did not lead to substantial improvements of the reconstructions. The spatial analyses of all five networks are shown in Figure A1 in ~~the~~ Appendix A for the annual evaluation.

Further, the persistence of day-to-day temperature variability is slightly underestimated in the reconstructions compared to the original grid (Appendix, Fig. A3) with differences in the autocorrelations reaching up to 0.15 for the sparse networks. Especially in the alpine areas, autocorrelation at lags of up to 10 days is lower than in the original grid. This can be related to the network density and setup. The scarcer networks have lower autocorrelation values in the areas with very few observations.

These spatial and seasonal differences may be related to the sparse and ~~uneven~~ unevenly distributed station network and the seasonal meteorological situations typical for Switzerland. In the winter half-year (October to March) during calm flow ~~situation~~situations, radiation fog and lifted fog (i.e. low stratus clouds) is a frequent phenomenon in the Swiss Plateau (Scherrer and Appenzeller, 2014). Such situations block direct radiation leading to ~~significant~~ significantly lower temperatures below the cloud layer. Because temperature data was mainly available in the Swiss Plateau below this inversion layer, a too cold day for the Alpine area may be selected as an analogue day and the temperature assimilation may be too cold because to Alpine inversion layer is not well captured. An evaluation of fog days showed these large biases for the Alpine area (not shown). This is confirmed by the biases seen in Figure 3k to o and would also lead to lower correlations and MSESS, and larger RMSE. The overall better performance in summer compared to winter for all networks (Fig. 5a and b) can also be related to such badly captured inversion layers, which are not present in summer months. For a reconstruction of monthly temperature, Isotta et al. (2019) found that the magnitude of the warm anomalies in the areas above the inversion is not reproduced if only a few stations are available in the Alpine regions. For the network with only 11 stations (Fig. 1a), the temperature bias in winter is actually smaller compared to the network with 21 and 32 measurements (Fig. 1b and c). Network two and three already contain the German station in Hohenpeissenberg at an altitude of 995 msl and they also have more stations in the Swiss Plateau. A wrongly captured inversion layer because of the station distribution may also cause a larger bias.

The cross-validation of the precipitation reconstruction shows a lower performance compared to deseasonalized temperature (Fig. 5 and 6). Spearman correlations range between 0.39 and almost 1 for all seasons and the annual evaluation considering the network with 32 measurements (Fig. 5c). The Alpine region does not stand out as pronounced as for the temperature validation. However, ~~in~~ southern Switzerland, the Ticino, and the southern Grison valleys do have correlation values of only 0.35. In contrast to temperature, correlations are generally higher for winter than for summer months. RMSE range between 3.09 and 26.89 and ~~are highest during~~ is highest during the summer months in Ticino. The Brier score is close to 0 around the locations, where precipitation occurrence is registered and decreases with distance. As for the other metrics, especially in the summer months, southern Ticino and southern Grison have very low values. The mean bias in all seasons is close to zero, because we conducted a quantile mapping taking into account the annual ~~precipitation differences~~ cycle of precipitation differences between the reconstruction and the original dataset (Fig. 5p to t).

With respect to the intensity of events in winter, days with more precipitation on an area-wide basis show higher correlations than days with less precipitation (Fig. 4c). In summer, spatial correlations do not vary in the median with respect to the area
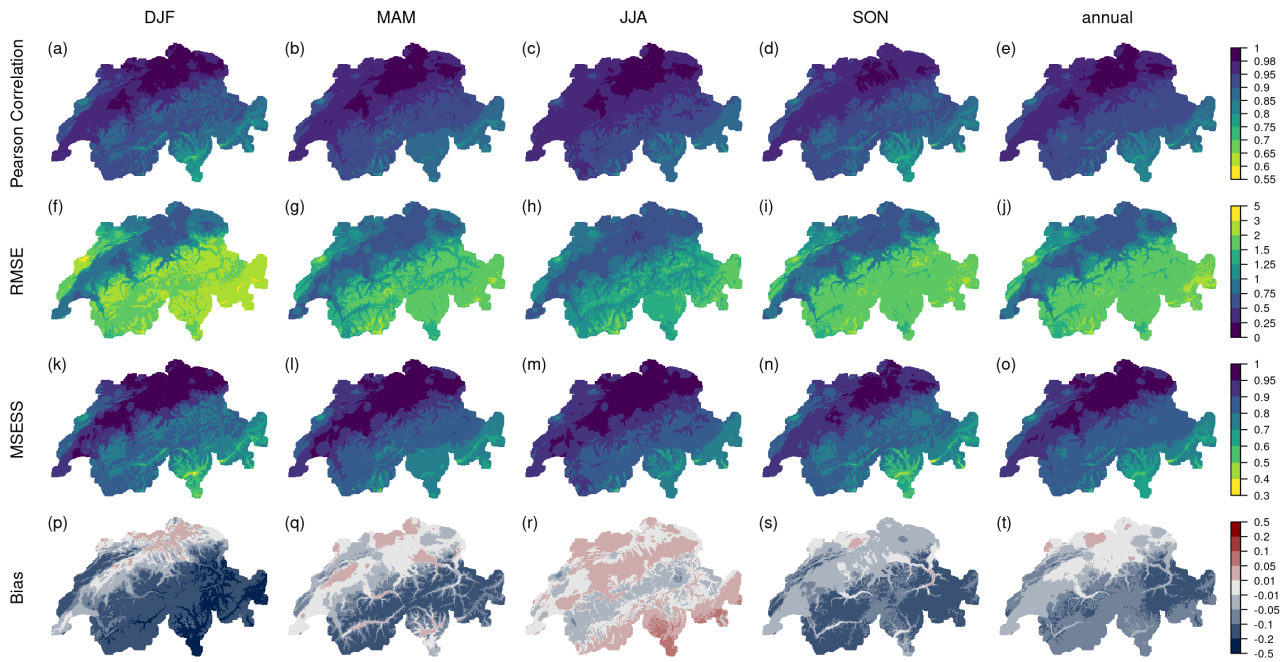
Figure 3. Cross-validation results of a network of 32 stations as in Fig. 1c for temperature anomalies during 1961-2020 for the four seasons (DJF, MAM, JJA, SON) and annually. a-e) Pearson correlation, f-j) RMSE, k-o) MSESS, and p-t) mean bias.

average intensity, however, the spread of the correlation increases for days with higher total precipitation. As to be expected, the ~~RMSEs increase~~ RMSE increases with increasing intensity of a rainy day. Especially in summer, the RMSE can reach very high values for the strongest events~~, whereas at~~. For higher altitudes, the values are even larger. These high values come from an underestimation of the strong precipitation events in both winter and summer, which is shown in the lowest row. Despite the bias correction, extreme precipitation is underestimated in the reconstruction of up to a median of 10 mm.

Differences between the networks are substantial for summer and winter (Fig. 5c and d), but the performance is generally better in winter than in summer. The ~~thinnest~~ sparsest network has a median correlation of 0.68, which increases considerably when stations are added. For the two networks after 1864 however, no more substantial changes occur. RMSEs are between 3.09 to 29.45 mm for the three networks of the early period and between 1.72 and 12.74 mm afterwards in winter. For the summer season, they are almost twice as large. For the annual evaluation of precipitation, the spatial analyses of all networks are shown in Figure A2 in the Appendix A.

~~The lower~~ Also, the persistence of dry and wet spells is underestimated in the reconstructions, however only slightly and with regional differences (Appendix Fig. A4). The fraction of dry (wet) days followed by dry (wet) days is up to 0.14 smaller in the reconstruction compared to the original data. The underestimation of the wet days persistence is largest in the Ticino and for the sparse networks, indicating that wet spells are less well captured. For the dry day persistence, no spatial pattern

14
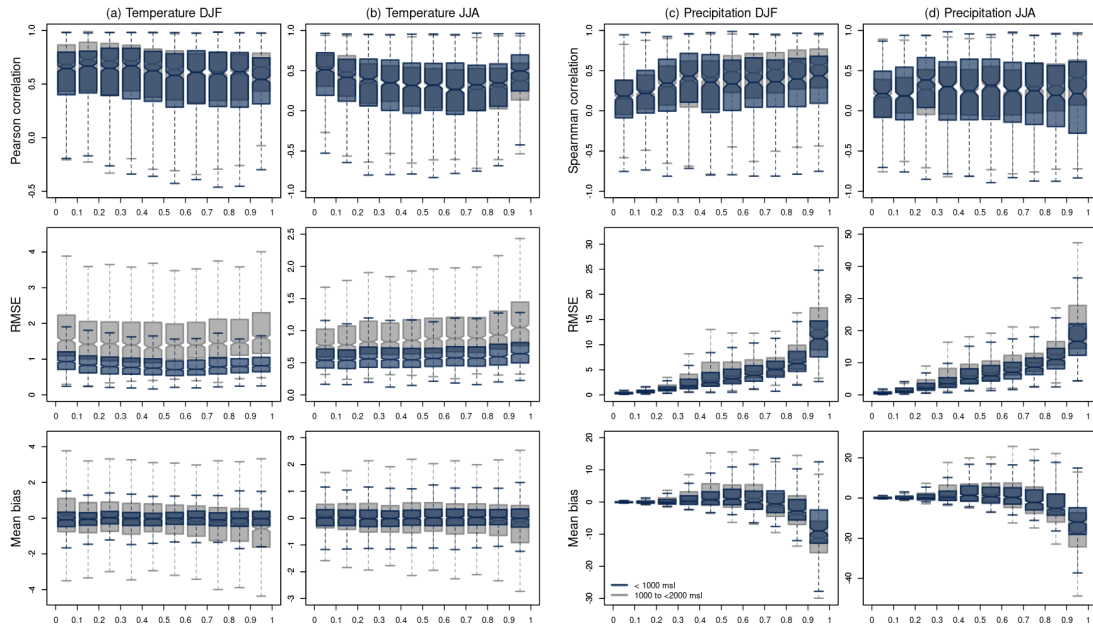
Figure 4. Spatial evaluation of the reconstruction ordered according to the deciles of the area mean between 7.4 to 9.1° E and 46.5 to 47.3° N for the original data set. a-b) DJF and JJA temperature evaluation with removed seasonality for Pearson correlation, RMSE, and mean bias. c-d) DJF and JJA precipitation evaluation for Spearman correlation, RMSE, and mean bias. Blue values show all grid cells below 1000 msl, grey values show grid cells above 1000 msl. The boxes range from the first to the third quartile, and whiskers extend to 1.5 times the interquartile range outside the box.

is visible. A lower persistence for both wet and dry days in the reconstruction can be expected since the analogue resampling
390 does not consider temporal information.

The lower performance of the precipitation reconstruction can be expected, since precipitation is a much more heterogeneous variable than temperature on a daily timescale impeding daily reconstruction, especially when only very few precipitation data are available. The performance differences in the reconstruction between winter and summer can be related to the type of precipitation occurring in these seasons. In summer, precipitation can be convective and very local, while in winter, precipitation is
395 often stratiform, covering larger areas. This ~~stratifrom~~ stratiform precipitation is easier to reconstruct. The Brier score decreases faster around the stations in summer than in winter. The poor performance in the Ticino and south-eastern Grison valley with large RMSEs may come from convective or orographic precipitation not being captured at all in the precipitation data covering only northern Switzerland. But also intense precipitation events are difficult to capture in northern Switzerland (Fig. 4c and d). In contrast to Pfister et al. (2020), the mean bias of the uppermost percentile (Fig. 4c and d, lowest row) is on average negative,
400 i.e. the reconstructed values are too low compared to the original. This may be because very few precipitation measurements enter the reconstruction and thus days with high precipitation are not ~~necessarily~~ selected from the analogue pool.

15
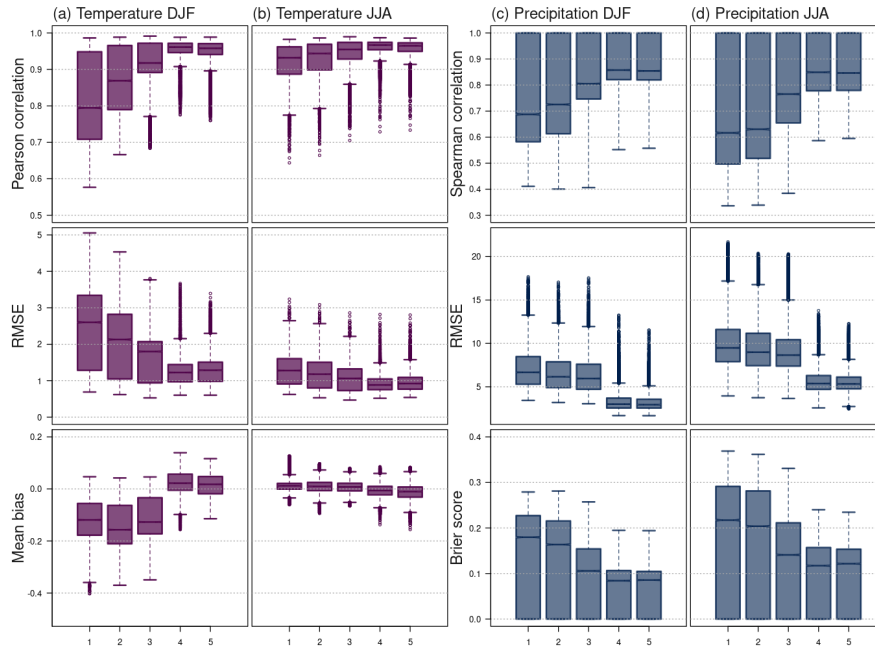
Figure 5. Cross-validation results for the five networks shown in Figure 1 for temperature anomalies during 1961-2020 a) in winter (DJF) and b) summer (JJA) showing Pearson correlation, RMSE, and mean bias and for precipitation c) in winter (DJF) and d) summer (JJA) showing Spearman correlation, RMSE, and Brier score.

The cross-validation results give us an impression of the performance of our reconstruction. However, they have some limitations. The cross-validation was performed based on station data in the reference period. These measurement data have a much higher quality than what we know from early instrumental data (see section 2.1). Further, our analogue pool is covering the same period as our reconstruction period. Therefore, it covers the same longer-scale variabilities, but not necessarily the same as they occur in the early period between 1763 to 1863. With respect to temperature, we calculated an offset in order to account for the climatic change between the 18th century and the late 20th and early 21st centuries. ~~It was~~ This offset is based on a state-of-the-art data set, but may not be accurate for the small and topographically heterogeneous area of Switzerland, thus adding an additional source of errors to the reconstruction.

4.2 Evaluation with independent data

A comparison with independent observations allowed us to assess the performance of the reconstruction in the reconstructed period itself, but the quality of the observations has to be considered. Temperature observations with removed seasonality in Aarau, Fribourg, Herisau, and Tegerfelden show Pearson correlations mostly above 0.85 ~~.~~ (Fig. 7a to d). Nufenen, Bellinzona, and Luzern show considerable lower values. The same pattern is also seen for the MSESS. RMSEs range between 1 to 4° C. Again, Aarau, Fribourg, Herisau, and Tegerfelden, have the smallest errors. The mean bias based on absolute values is mostly

405

410

415

16
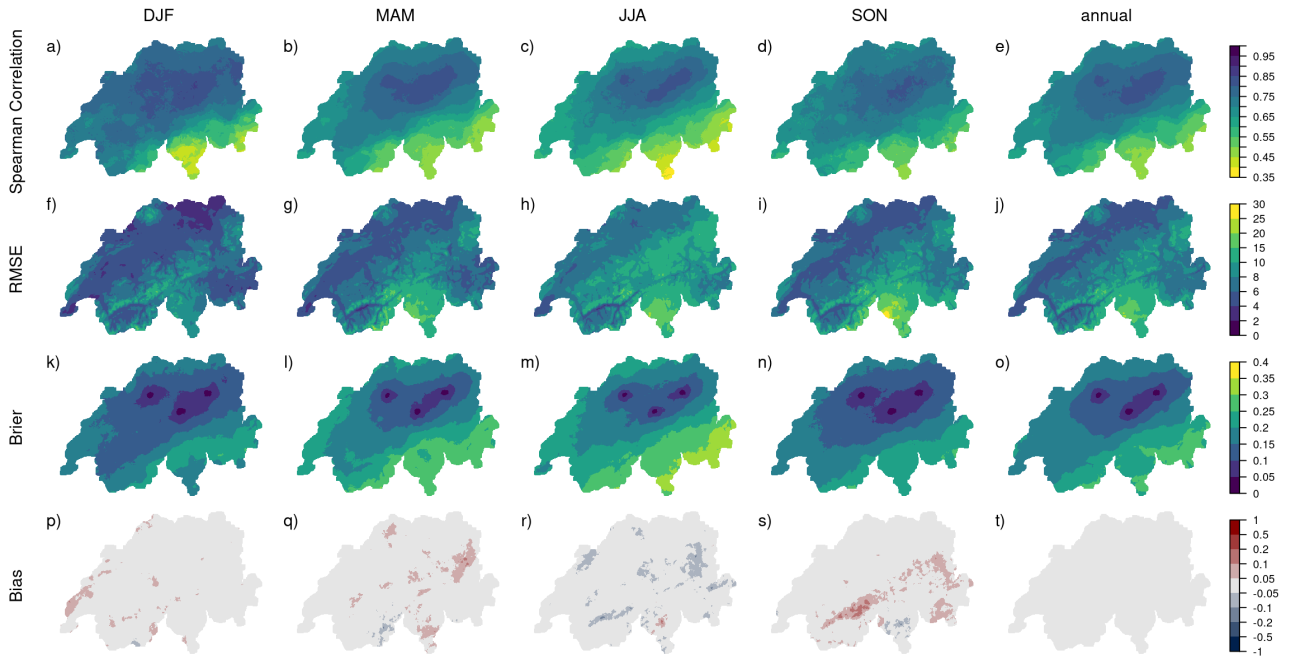
Figure 6. Cross-validation results of a network of 31 stations as in Figure 1c for precipitation during 1961-2020 for the four seasons (DJF, MAM, JJA, SON) and annually. a-e) Spearman correlation, f-j) RMSE, k-o) Brier score, p-t) mean bias. The RhiresD data set contains in addition to Switzerland also the northern catchments.

between ~~0~~ 2 to 2° C for Fribourg, Herisau, and Tegerfelden. For Bellinzona, Luzern, and Nufenen, the reconstruction shows colder values than the observations in all seasons.

Fribourg, Herisau, Tegerfelden, and Aarau are all located in areas with a high station density (see Fig. 1). This contributes to the better performance of the reconstruction in these areas, but their good agreement confirms that for the Swiss Plateau our reconstruction provides useful results. Nufenen and Bellinzona show the lowest correlation values and the largest biases. For Bellinzona, Brönnimann and Brugnara (2022) showed that the subdaily measurements in July are considerably warmer than what is expected from the daily cycle representative for this area, most likely because of radiative biases. This would explain that the reconstruction is colder than the observations, which is especially pronounced in summer (Fig. 7e). Furthermore, Bellinzona lies in an area with no close-by observations used in the reconstruction. Due to that we would expect cold mean biases for winter as seen in the cross-validation, but not for summer (Fig. 3). For Nufenen, the closest grid cell in the reconstruction corresponds to an altitude of 1866 msl, whereas the village Nufenen, where the measurements were taken, is at 1580 msl. 300 m of altitudinal difference can thus explain the large negative biases found between observation and reconstruction.

~~A~~ For precipitation, a comparison with independent ~~precipitation~~ observations is only possible for a series of precipitation occurrence in Bern between 1807 and 1818. Based on the cross-validation, we can expect a Brier-score between 0.15 and 0.2 (i.e. up to 20 % of the days are wrongly assigned to a wet or dry day) for this location and the respective network. The Brier-

17

score between the closest grid cell in Bern and the precipitation occurrence series from weather notes yields 0.25 0.24, thus, higher than the cross-validation results. However, we compare ~~in that case~~ a station measurement with a grid cell (of 1x1 km) covering a slightly different scale. Also, precipitation occurrence may have a problem with accounting night time precipitation correctly for the exact day of the weather notes. The gridded data are a daily sum between 6 am in the morning and 6 am the next day, while this may not be entirely clear for the weather notes. Figure 7f shows precipitation occurrence for a dry (1811) and very wet year (1816). Long-lasting dry spells such as in March and April 1811 are captured by the reconstruction, as well as the overall wet summer of 1816, but for individual days, reconstructions deviate from observations. This is also seen in the comparison of monthly wet-day-frequency from the reconstruction and observation (Fig. 7g) which agree overall well (Pearson correlation of 0.83 0.84).

4.3 Assessment of long-term variability

The 258-year-long daily reconstructions should reproduce daily weather as well as long-term variability of temperature and precipitation over Switzerland. We assess this long-term variability by comparing the field mean of our data set to other data sets covering the same or similar periods (Valler et al., 2022; Casty et al., 2005). These data sets are not independent and consist either of only observations, statistical reconstructions based on proxy data and observations, or reanalyses.

The annual temperature anomalies with respect to the 1871 to 1900 climatology agree well in all data sets for the reconstruction period from 1864 to 2020 (Fig. 8a). This period has good coverage of temperature data with high quality and thus, a good agreement can be expected. Only the reconstruction by Casty (Casty et al., 2005) is colder in the first half of the 20th century. Also, the data sets with a lower spatial resolution (EKF400v2, Casty) do not capture the steep warming at the end of the 20th century. Before 1864, deviations between the data sets are larger. The annual mean of the Swiss reconstruction is up to 0.5 ° C warmer than EKF400v2 and the Swiss Plateau series before 1800. The temperature differences are larger in winter than in summer (not shown). There are several reasons, that might lead to the warmer temperatures in the Swiss reconstruction. EKF400v2 is used for homogenization and for calculating an offset between the reference period and the historical period. This offset might be too small especially in winter since EKF400v2 is colder than the Swiss data in winter in the reference period.

The agreement between precipitation reconstruction is much lower (Fig. 8b). After 1864, all data sets reproduce similar patterns, however with different magnitudes. Differences in the anomalies reach up to 3 % when comparing our reconstruction to RrecabsM1864 (MeteoSwiss, 2021c). Before 1864, differences among the data sets are considerable. Whereas the reconstruction of Casty partly agrees in terms of the direction of the signal with the Swiss reconstruction, EKF400v2 does not agree at all. Also, the Swiss reconstruction is on average drier before 1864 compared to the period after 1864. The smoothed time series only shows periods (around 1770 and 1850) with wetter conditions than the average from 1871 to 1900. Since very little information on absolute precipitation enters the reconstruction, and the bias correction might not fully correct the dry bias, a too dry reconstruction can be expected. However, individual years, such as the year without summer 1816 (Luterbacher and Pfister, 2015, e.g.) and the wet summer of 1770 (see next section), do show large positive precipitation anomalies (Fig. 8b and Fig. A5d). The precipitation reconstruction, therefore, needs to be used with care. Also, note the
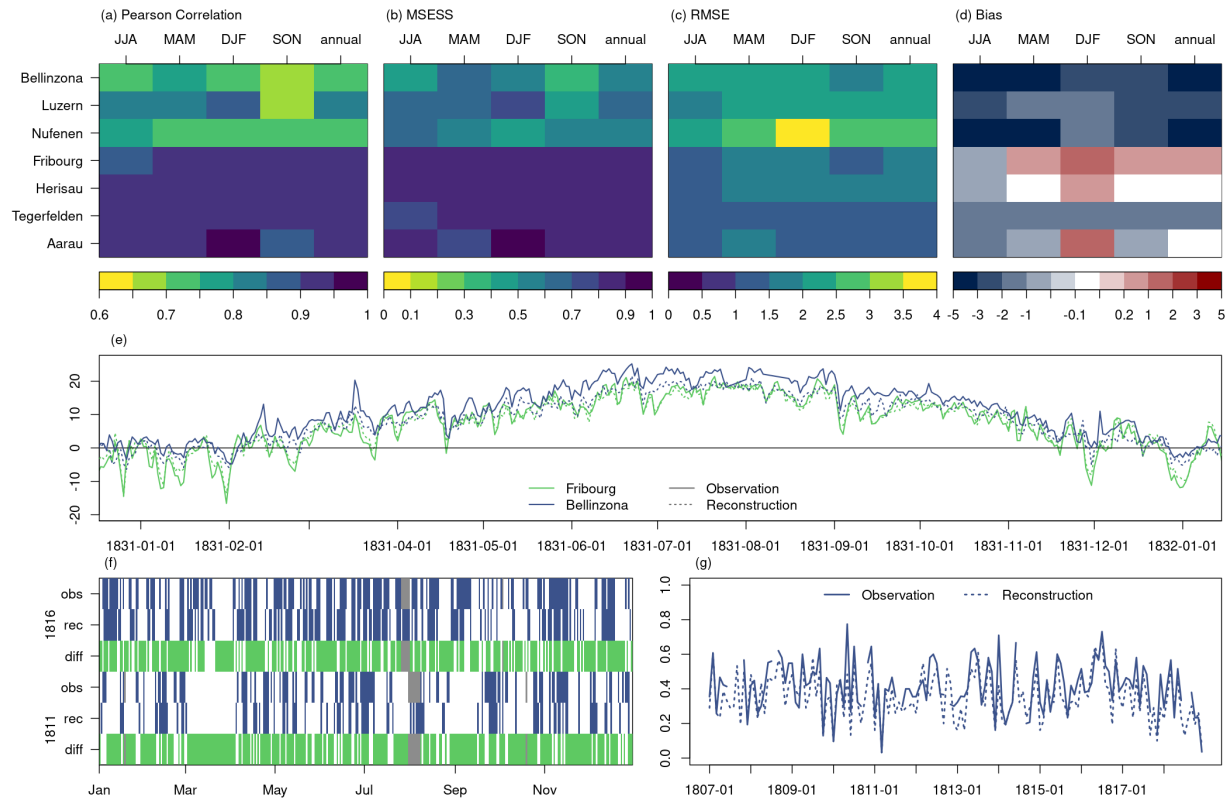
Figure 7. Evaluation of the closest grid point from the reconstruction and the observations for values with removed seasonality. a) Pearson correlation, b) RMSE, c) MSESS, and d) mean bias. Each box shows the four seasons and annual values on the top x-axis and the different locations on the y-axis. Locations are marked with an asterisk in Fig. 1a. e) Time series of two observations in Fribourg and Bellinzona and the closest grid points of the reconstruction for the year 1831. f) wet days for the observations from weather notes in Bern and reconstruction for two years 1811 and 1816. A wet day is marked with a blue bar and a missing observation is marked with a grey bar. Green bars show the days that are correctly assigned to wet and dry. g) Comparison of monthly wet day frequency for the period 1807 to 1818 for the data from f).

465 main aim of the reconstruction was to create daily fields rather than creating a reconstruction with good long-term consistency. This needs to be considered when using the dataset.

5 Case study: The European famine years 1770 to 1772

During the years 1770 to 1772 Central Europe was hit by a severe famine which was considered one of the most devastating socio-ecological extreme events of the little ice age. According to Collet (2018), the famine may have been of similar magnitude

470 as the famines of the 1315s and 1570s, causing hundreds of thousands of deaths. The crisis was related to long-lasting wet and
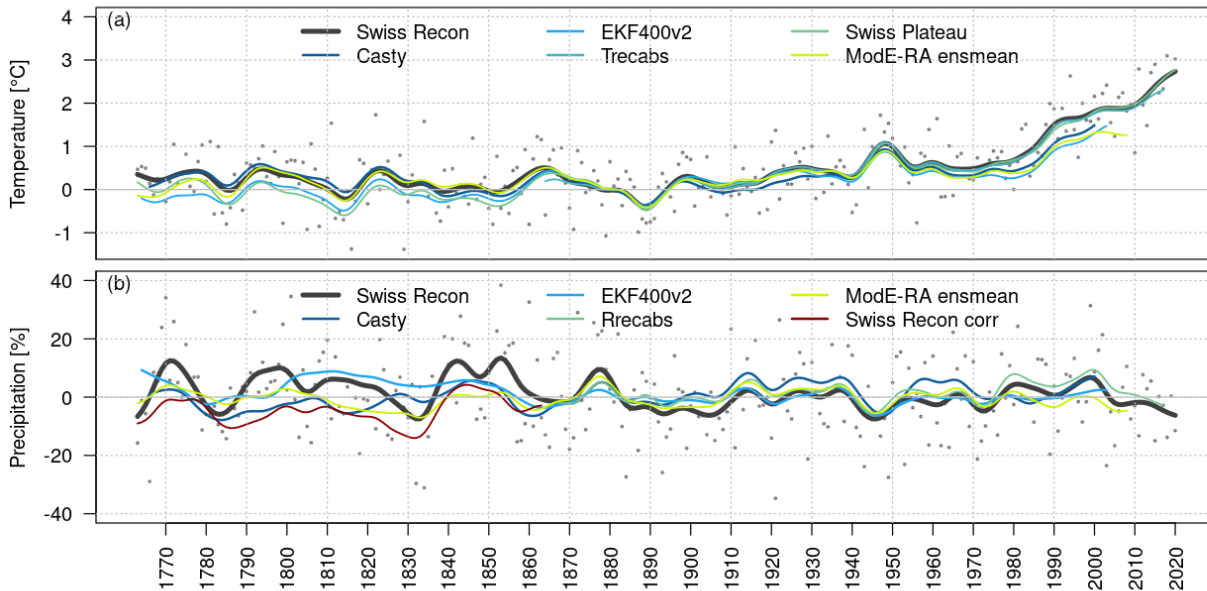
Figure 8. a) Long-term evolution of annual temperature anomalies in different data sets. b) Long-term evolution of annual precipitation anomalies as % deviation from the mean. The time series are smoothed with a Gaussian filter (sigma = 3). Grey dots show reconstructed annual anomalies. All anomalies are calculated with respect to the 1871-1900 climatology for each data set. The time series either represent the field means (Trecabs/Rrecabs, Swiss reconstruction) or the closest grid point of the data set. The Swiss Plateau time series is based on the Bern and Zurich series as described in (Brugnara et al., 2022).

cold conditions between 1769 to 1772 from France to Ukraine and Switzerland to Scandinavia. It hit a society with low coping capacities, and a very high ~~cereal-dependence~~ cereal dependence beyond mere consumption; cereals were the key staple food ~~,~~ but served as well as means of payment and taxation. This "cereal society" in Europe was highly vulnerable to adverse weather conditions, especially during the summer months. In the Czech ~~republic~~Republic, around 10 % of the population died due to

475   ~~the~~ consecutive crop failures in the third year of the famine from 1771 to 1772 (Pfister and Brázdil, 2006). In contrast, for Switzerland, Pfister and Brázdil (2006) demonstrated that despite a loss of harvest, the famine was less severe due to a low social vulnerability by contemporary standards, effective interventions by the state, and because the climate anomaly affected only two harvests.

Collet (2018) summarised data from societal and natural archives describing the climate anomaly across Europe. According

480   to him, the devastating impacts of the adverse weather ~~was~~ were related to its length rather than its magnitude. In fact, it has not been shown to be an outstanding climate anomaly with respect to magnitudes of temperature and precipitation anomalies in climate reconstructions (Luterbacher et al., 2004; PAGES2kConsortium, 2013; Pauling et al., 2006). A composite of 1769 to

20

1771 from the old world drought atlas shows however very wet conditions mainly for a limited area of south-eastern Germany, northern Austria, and western Czech republic (Cook et al., 2015).

485 For Switzerland, we summarized documentary sources that reported on the wet and cold weather conditions and on related impacts for the summer-half year of 1770 (Table 3). These reports include for example late snowfall, continuous snow cover, rain and flood impacts, and poor harvests. With our reconstructed daily fields, we tried to confirm the described long-lasting wet and cold conditions. However, particularly the lack of precipitation observations in the reconstruction has to be kept in mind.

490 The area mean of the Swiss reconstruction indeed shows monthly precipitation anomalies (with respect to the 1763 to 1812 climatology) which are constantly above average for a period from 1769 to the end of 1771 (Fig. 9a). Two other data sets EKF400v2 (Valler et al., 2022) and Casty (Casty et al., 2005) show peaks in 1770 and 1771, but not the persistent positive precipitation anomalies. Note, that we use a 12-month running mean for the time series shown and that we select the closest grid cells in EKF400v2 and Casty. Thus, the data are not representative ~~for~~ of exactly the same area. Temperature anomalies

495 are negative especially for the first half year 1770, but also for the beginning of 1771 (Fig. 9b). For temperature, the three data sets agree well, which is not the case for precipitation. For precipitation, however, the data sets agree better starting in the 19th century (not shown).

Crop failure mainly relates to adverse weather conditions during the growing seasons. To track these adverse weather conditions, we exemplary have a look at the summer half-year 1770. Several sources report on abundant snowfall for the month

500 of April 1770 (Table 3) which may have delayed the start of the growing season. Days with snowfall were calculated using a threshold of 2° C for daily mean temperature ~~(Zubler et al., 2014) and 0.1~~ and 1 mm for precipitation ~~, which is our wet-day definition~~ as it has been derived by Zubler et al. (2014). Optimal temperature thresholds for distinguishing snow from rain, however, heavily depend on the relative humidity of the air, which we do not have as a parameter for the historical time period, and they depend on the season (Jennings et al., 2018; Kienzle, 2008). Large parts of Switzerland show above average number

505 of days with snowfall with respect to the 1763 to 1812 April climatology (Fig. 10a). In the Pre-Alps and the Jura, up to 12 days more snowfall occurred than on average. For the surrounding hills of Bern and Gurzelen, for which historical sources reported snowfall, up to 3 snowfall days more occurred than usual, which is in relative terms almost a doubling with respect to the April climatology. At lower elevation areas in the Swiss Plateau, low elevated mountain valleys, and the Ticino no snow days were registered in the reconstruction. For example, for Basel, weather notes by d'Annone (Brönnimann and Brugnara, 2020a) note

510 snowfall for four days, but from our reconstruction no snowfall can be inferred. However, using daily data for snow detection is difficult, as the threshold for snow to occur may be reached at some point during the day, whereas it is not reached based on the daily mean, particularly so in spring. Indeed, daily temperature values in Basel by d'Annone never reached values below 2.5° C. However, the early morning measurements reached for example 1.6 and 1.9° C on the days when snowfall was reported.

Crops ~~need~~ require a certain amount of ~~energy in the form of temperature~~ accumulated heat to reach their different pheno-

515 logical stages. ~~This energy amount can be summarized in~~ The growing degree days (GDD) ~~, which is a~~ index can be used to express this heat accumulation needed until a phenological stage is reached (Wypych et al., 2017). The index is calculated as the sum of daily mean temperature above a certain threshold of daily mean temperature (e.g. Bonhomme, 2000). ~~To look at~~

the growing season, commonly a threshold of ~~the growing season, commonly a threshold of~~ Here, we set this threshold to 5° C ~~is used (Wypych et al., 2017)~~. At a GDD of 1000° C, various cereals, such as oat, barely ~~or~~ and wheat, reach their ~~seed filling~~ seed-filling phase (Miller et al., 2001). In the

520 summer 1770, a ~~1000 GDD~~ GDD of 1000 ° C was reached in the Swiss plateau around 15 days later ~~and for higher altitude locations up to 30 day later~~ than what would be expected on average for the period from 1763 to 1812. ~~The 1000 GDD~~ For higher altitude locations it was reached even up to 30 days later. This growth stage was therefore delayed by around half a month in the year 1770 (Fig. 10a). However, also the weather conditions at later stages are relevant for plant development and harvest. In the summer half-year 1770, the ~~amount~~ number of cold days was increased, which can be seen in the anomaly of

525 a cold days index, i.e. the number of days below the 20th quantile calculated for each day of the year. It shows mainly for the area north of the Alps above average cold days ranging from +5 to +30 days (Fig. 10b). In southern Switzerland, this was less pronounced and only between 0 to 10 more cold days were registered.

Historical sources also reported ~~about~~ the wet conditions throughout the summer, for example for the Bodensee and the Rheintal (see Table 3, ~~Paffrath (1915) and Walser (1731)~~Paffrath (1915) and Walser (1731)). For the summer season from April

530 to September 1770, in most of northern Switzerland above average wet-days were recorded with areas reaching up to 125 % wet days compared to the climatology of 1763 to 1812 (Fig.10c). In the very south of southern Switzerland, also above average number of wet days were recorded, although some areas also show around average number of wet day. These values thus confirm the reports of ~~wetter than usual~~ wetter-than-usual weather.

However, if we compare the summer of 1770 to the summer 1816 in our reconstruction, which is known for its very wet and

535 cold conditions as "the year without a summer" (Flückiger et al., 2017; Luterbacher and Pfister, 2015), these anomalies become small (see Appendix, Fig. A5). In 1816, a GDD of 1000 was reached on the Swiss Plateau on average 20 to 25 days later. The area ~~,~~ where a GDD of 1000 is never reached ~~,~~ is much larger, meaning, that some cereals never fully developed. Up to 50 more cold days were registered during the summer 1816, and wet days increased to up to 150 % compared to the 1763 to 1812 climatology. The summer 1816 was, therefore, considerably more extreme. Our reconstruction might also be more accurate for

540 the summer 1816, particularly for precipitation, as up to four precipitation/precipitation occurrence time series were available ~~for~~ in 1816 and also considerably more temperature measurements.

With the reconstruction, we are nevertheless able to reproduce the wet and cold weather during 1769 to 1771 ~~for~~ in Switzerland, which had caused severe famines in parts of Central Europe. Studies showed that based on such gridded data sets for example crop yields (Flückiger et al., 2017) can be simulated. Such follow-up studies could also be applied to quantitatively

545 reproduce crop losses for this famine, for Switzerland based on the here presented reconstruction, or even for ~~entire~~ the entire of Europe.


6 Conclusions

In this study, we present a reconstruction of ~~around 250~~ 258 years of high-resolution daily temperature and precipitation fields for Switzerland covering the period 1763 to 2020. The data set is available at the open-access repository PANGAEA

550 (~~provisional link:~~ https://doi.pangaea.de/10.1594/PANGAEA.950236) (Imfeld, 2022). Meteorological fields were resampled
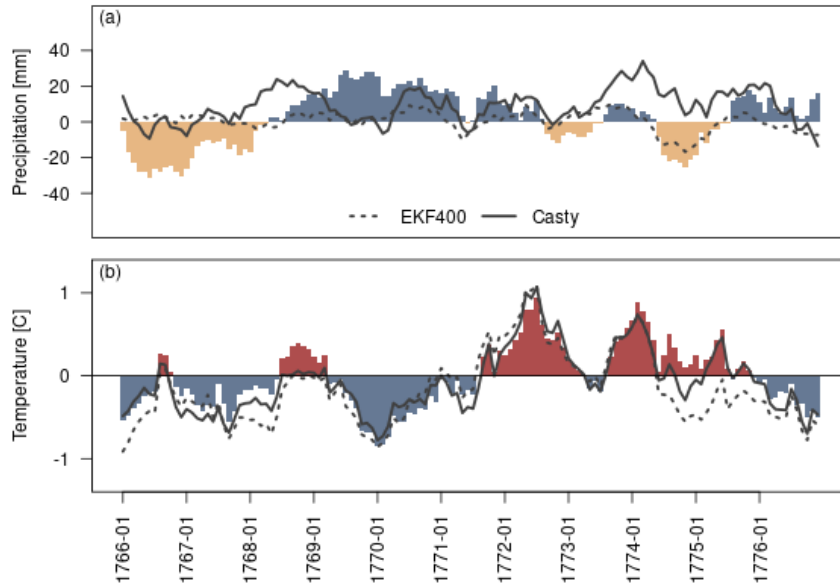
Figure 9. a) Area mean of monthly precipitation anomalies with respect to the monthly 1763 to 1812 means for the precipitation recon-struction (coloured bars), lines show the closest grid point of EKF400v2 (dotted) and of the reconstruction from Casty (solid). b) Area mean of monthly temperature anomalies with respect to 1763 to 1812 for the temperature reconstruction, lines show the closest grid point of EKF400v2 (dotted) and the reconstruction from Casty (solid). All values are a mean over a 12-month window.
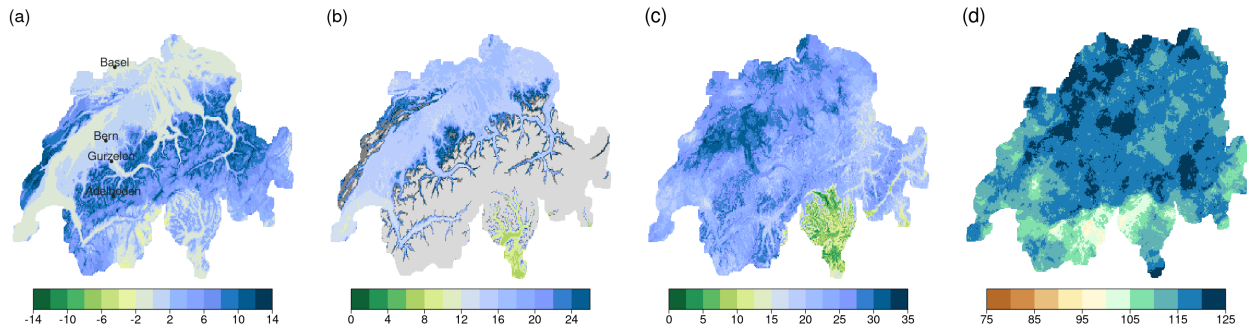
Figure 10. a) Anomaly of the number of days with snowfall for April 1770. Black dots denote areas where abundant snowfall was reported in historical sources. b) Anomaly in days for the year 1770 when the threshold of 1000 GDD was reached. Light grey areas denote values where no climatology of a 1000 GDD threshold was calculated because the threshold was reached in less than 75 % of the years between 1763 to 1812. Dark grey denotes areas where the threshold of 1000 GDD was not reached in the year 1770. c) Anomaly of number of cold days (days below the 20th percentile of daily mean temperature) for April to September 1770. d) Wet-days anomaly in percentage for April to September 1770. All anomalies are calculated with respect to the 1763 to 1812 climatology.

based on the most similar days in a reference period calculated from station measurements. The resampled temperature fields were further improved with data assimilation and the resampled precipitation fields were bias corrected with quantile mapping. Extending a daily reconstruction for Switzerland as far back as the end of the 18th century was possible because of the data rescue efforts of the CHIMES and follow-up projects (Brugnara et al., 2020b; Pfister et al., 2019; Brugnara et al., 2022).

555 Despite the considerable decrease ~~of~~ in observations before 1864, the reconstruction still shows good results. Pearson correlations from a cross-validation of deseasonalized temperature are between 0.58 to 0.99 and RMSEs up to 5° C including the very scarce network set-ups. Because very few or no station observations are available for the Alps and the south side of the Alps, the performance is considerably reduced in these regions. Cross-validation results for precipitation show lower performance than for temperature because few precipitation data were available and because precipitation is highly heterogeneous in space. The use of weather notes transformed to precipitation occurrence increased, however, the Spearman correlation and Brier score, especially around the measurement locations, but it decreased rapidly with increasing distance from the observations.

The validation with independent station data confirmed the better reconstruction skills for temperature for stations in the Plateau region and worse results for stations in the Alps. A comparison to an independent time series of precipitation occurrence showed that around 76 % of the days are assigned to wet or dry days correctly ~~,~~ and that the reconstruction was able to reproduce the monthly wet-day frequencies, indicating that the few observations of precipitation occurrence helped to reconstruct the monthly signal.

However, ~~some~~ several limitations have to be considered, when working with the data set. The results of the cross-validation cannot directly be used to infer the reconstruction skill in the historical period, because the data quality differs and data gaps in the historical period have not been filled. Early instrumental data are a valuable source of information on daily weather in the 17th, 18th, and 19th century~~. However,~~, but it comes with uncertainties that are often hard to correct. A reconstruction based on such data inherits these errors and uncertainties. Also, the method assumes that our analogue pool represents the weather of the previous 200 years, but the 60 years of our analogue pool may not cover enough extreme events, which we are thus not able to reconstruct. Furthermore, the lack of stations south of the Alps and in the Alps considerably lower the reconstruction quality in these areas. Reconstruction errors were large in the south of Switzerland especially for precipitation, because the Alps act as a climatological barrier. Measurements would be needed to create a valid reconstruction for this area. Lastly, the changes in the network introduce inhomogeneities that need to be considered when working with long-term data.

Nevertheless, our case study on the famine years 1769 to 1772 shows that the wet and cold weather described in various documentary sources are reproduced in the reconstruction. The summer of 1770 was~~for example~~, for example, wetter and cooler than average, but it did by far not reach the wet and cold conditions of the summer of 1816 in Switzerland. The new reconstruction also opens options to study similar events in more detail, for example by feeding the reconstructed fields into crop models or hydrological models.

Further ~~improvement~~ improvements of the data set could be obtained ~~on the one hand through~~ by incorporating more and ~~better corrected~~ better-corrected data. Especially, the long time series such as they have been created for Bern, Basel, Geneva, and Zurich (Brugnara et al., 2022) are very valuable. Despite being very tedious work, ~~especially~~ the precipitation reconstruction could profit substantially if more weather notes were digitized. Other reconstruction approaches have been and are being

24

explored, that could also contribute to improved reconstructions~~based on~~, for example machine learning techniques and data assimilation for precipitation, as well as methods including temporal information in the reconstruction. Furthermore, for some applications, not only daily mean temperature, but also minimum and maximum temperature, and sunshine duration are needed ~~that can be reconstructed as well~~ and could be reconstructed in a similar manner since gridded data for a reference period are

590   available.

Appendix A
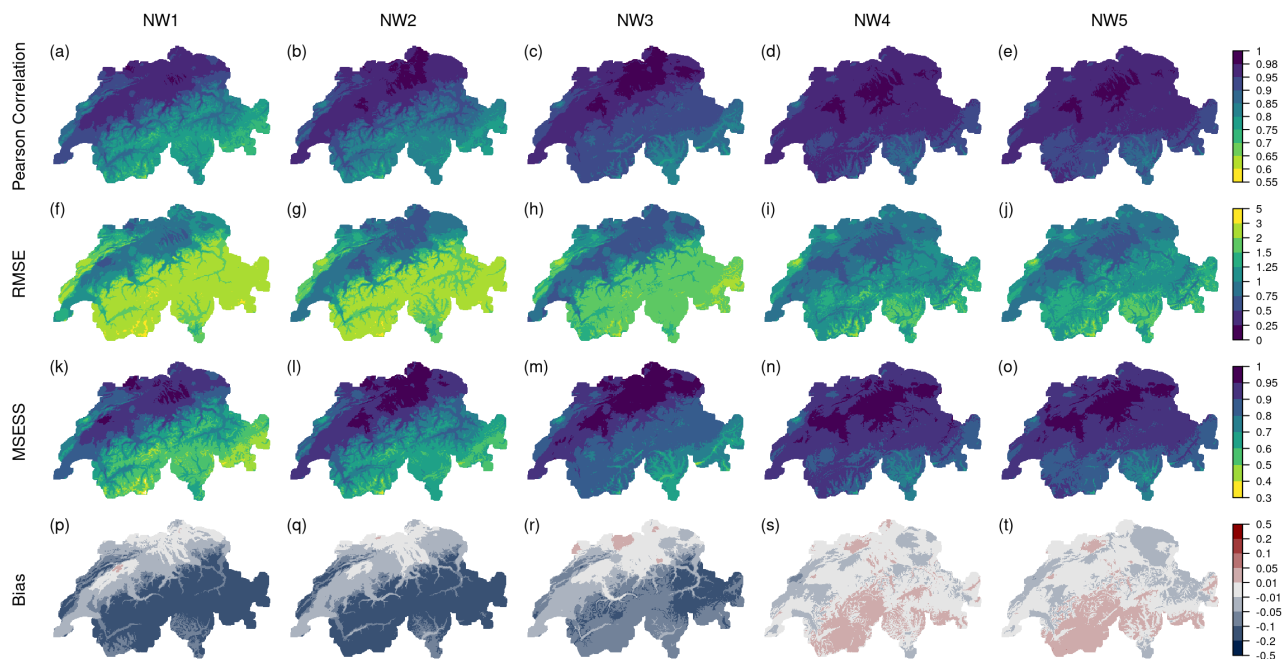
Figure A1. Cross-validation results of all networks shown in Figure 1a-e with 11, 21, 32, 43, and 108 time series used for reconstruction the precipitation fields. The cross-validation results are based on annual deseasonalized temperature anomalies during 1961-2020. a-e) Pearson correlation, f-j) RMSE, k-o) MSESS, and p-t) mean bias.

Table 1. Stations used for the reconstruction of the 1763 to 1863 period. The letters for the variables are p = pressure, ta = air temperature, rr = precipitation rate, rr0 = precipitation occurrence. A description of the CHIMES data set and where it is available is found in Brugnara et al. (2020b). If additional ~~evaluation~~ evaluations of the station exist, the respective reference is noted in the column "Hist Sources". For the reference data, MCH denotes station observations from the Swiss National Weather Service. For further abbreviations refer to Sect. 2.2.

ID	Station	Country	Lon	Lat	Alt	Variables	Hist Period	Hist Source	Ref Source
BAS	Basel	CH	7.588	47.558	253	p,ta,rr0	1763-1863	CHIMES Brönnimann and Brugnara (2020a) Brönnimann and Brugnara (2021)	MCH
BER	Bern	CH	7.452	46.948	554	p,ta,rr	1763-1863	CHIMES Brugnara et al. (2022)	MCH
BOL	Bologna	IT	11.353	44.497	-	ta	1763-1863	PALAEO-RA	EOBS
BUS	Aarau	CH	8.043	47.393	384	p,ta,rr0	1807-1863	CHIMES Faden et al. (2020)	TabsD, RhiresD MeteoSwiss (2021b, a)
ENS	Einsiedeln	CH	8.752	47.127	906	rr0	1817-1858	CHIMES	RhiresD
FON	Fontaines	CH	6.900	47.044	767	ta	1843-1862	Brönnimann and Brugnara (2022) CHIMES	MeteoSwiss (2021a) TabsD MeteoSwiss (2021b)
GOT	Gotthard	CH	8.568	46.555	2093	p,ta	1781-1792	CHIMES Brönnimann and Brugnara (2020a)	MCH
GSB	Gst Bernhard	CH	8.568	46.555	2093	p,ta	1817-1863	CHIMES Brönnimann and Brugnara (2020b)	MCH
GVE	Geneva	CH	6.143	46.204	411	p,ta,rr	1782-1863	CHIMES/Digihom Häderli et al. (2020) Brönnimann et al. (2020)	MCH
HOH	Hohenpeissenberg	D	11.020	47.800	995	p,ta	1781-1863	DWD Winkler (2006)	DWD
KAR	Karlsruhe	D	8.404	49.008	122	p	1778-1863	Palaeo-RA	ECA&D
LUZ	Lucerne	CH	8.404	49.008	122	p	??1778-1863	CHIMES Brönnimann and Brugnara (2022)	MCH
MIL	Milano	IT	9.180	45.470	132	p,ta	1763-1863	Improve	EOBS
NEU	Neuenburg	CH	6.930	46.991	434	p,ta	1763-1782	CHIMES Wyer et al. (2021)	MCH

Table 1. Continued.

ID	Station	Country	Lon	Lat	Alt	Variables	Hist Period	Hist Source	Ref Source
PAD	Padua	IT	11.870	45.400	31	p,ta	1766-1863	PALAEO-RA	ECA&D
ROV	Rovereto	IT	11.050	45.900	200	ta	1800-1839	PALAEO-RA	EOBS
SHA	Schaffhausen	CH	8.639	47.696	400	p,ta	1794-1845	CHIMES	MCH
SMA	Zurich	CH	8.538	47.370	410	p,ta	1763-1863	CHIMES Brugnara et al. (2022)	MCH
STG	St.Gallen	CH	9.379	47.425	676	p,ta,rr0	1813-1853	CHIMES Hürzeler et al. (2020)	MCH
TOR	Torino	IT	7.680	45.070	281	p,ta	1763-1863	Improve	EOBS (p) and ECA&D (ta)
VEV	Vevey	CH	6.844	46.460	378	ta	1805-1840	CHIMES Brönnimann and Brugnara (2022)	TabsD
ZUG	Zug	CH	8.515	47.166	424	ta	1843-1863	CHIMES Brönnimann and Brugnara (2022)	TabsD

Table 2. Stations used for independent evaluation of the 1763 to 1863 period from CHIMES. A description of the CHIMES data-set and where it is available is found in Brugnara et al. (2020b). If additional evaluation of the station exist, the respective reference is noted under "Hist Sources".

| CHIMES ID	Station	Country	Lon	Lat	Alt	Variables	Hist Period	Hist Source
BE01_Bern_Studer	Bern	CH	7.452	46.948	534	rr0	1807-1818	CHIMES
								Hari et al. (2022)
AG01_Aarau_Bronner	Aarau	CH	8.043	47.393	384	ta	1857-1865	CHIMES
								Faden et al. (2020)
AG02_Tegerfelden	Aarau	CH	8.285	47.559	364	ta	1843-1853	CHIMES
AR01_Herisau_Merz	Herisau	CH	9.279	47.385	770	ta	1821-1831	CHIMES
								Weber et al. (2020)
FR01_Fribourg	Fribourg	CH	7.158	46.807	627	ta	1829-1836	CHIMES
								Brönnimann and Brugnara (2022)
GR11_Nufenen	Nufenen	CH	9.245	46.539	1580	ta	1834-1846	CHIMES
LU01_Luzern_Ineichen	Luzern	CH	8.304	47.052	435	ta	1826-1832	CHIMES
								Brönnimann and Brugnara (2022)
TI02_Bellinzona	Bellinzona	CH	9.023	46.191	230	ta	1826-1832	CHIMES
								Brönnimann and Brugnara (2022)

Table 3. Selection of registered weather impacts from the wet and cold weather in Switzerland in the summer half-year 1770 based on own sources (Brugnara et al., 2020b) and Euro-Climhist (Pfister et al., 2017).

| Time	Location	Impacts	Source
Spring	Geneva	snow impact on agriculture	Piuz (1974)
April	Adelboden (BE)	abundant snow	Baertschi (1916)
April	Gurzelen (BE)	snow impacts on agriculture	Oekonomische Gesellschaft Bern, Metadata in Pfister et al. (2019)
April	Bern (BE)	snow impacts on agriculture	Oekonomische Gesellschaft Bern, Metadata in Pfister et al. (2019)
April	Bodensee	abundant rain, snowfall, hay prices increase	Paffrath (1915)
April/May	Appenzell-Innerrhoden	late snowmelt	Walser (1731) (source not entirely clear)
May	Uri	abundant snow	Schaller-Donauer (1937)
June/July	Gurzelen (BE)	fresh snow at higher elevations	quoted in Zumbühl (1980)
July	Bodensee	abundant rain, hail, rain impact	Paffrath (1915)
August	Bodensee	abundant rain, impacts of floods and high water level	Paffrath (1915)
Summer	Glarus	pasture yield poor: most mountain snow cover does not melt	Trümpi (1774)
Summer	Grindelwald (BE)	permanent snow cover	Strasser (1890)
Summer	Stockhorn Massif	permanent snow cover	quoted in Pfister (1975)
Summer	Rheintal (SG)	high water level	Walser (1731) (source not entirely clear)
September	Gurzelen (BE)	fresh snow at higher elevations	Oekonomische Gesellschaft Bern, Metadata in Pfister et al. (2019)
September	Erguel (BE)	production of vegetables/potatoes very poor	Kohler (1871)
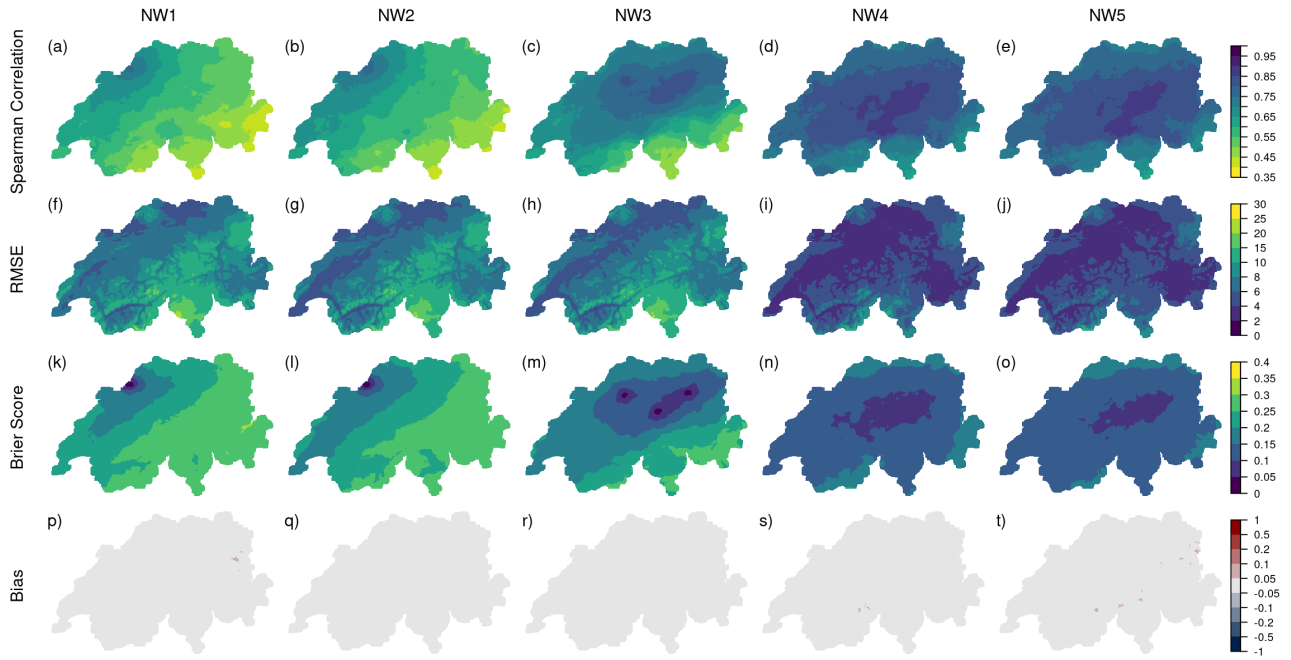
Figure A2. Cross-validation results of all networks shown in Figure 1a-e with 11, 21, 32, 43, and 108 time series used for reconstructing the precipitation fields. The cross-validation results are based on annual daily precipitation during 1961-2020. a-e) Spearman correlation, f-j) RMSE, k-o) Brier score, and p-t) mean bias. The RhiresD data set contains also the northern catchments that drain into Switzerland.
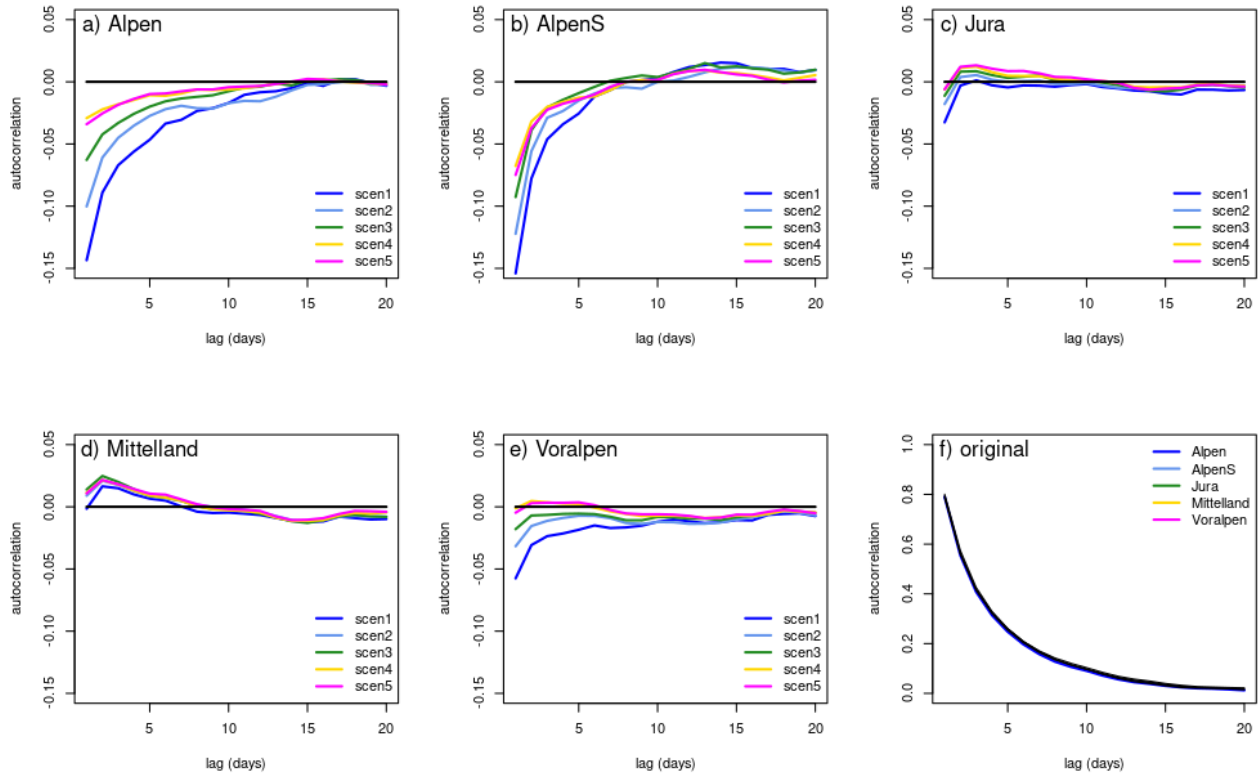
Figure A3. ~~a~~a-e) ~~Anomaly~~ Differences between the area mean autocorrelation of ~~number of days with snowfall~~ the original grid and reconstructed grid for ~~April 1816. b) Anomaly in days for~~ the ~~year 1816 when the threshold~~ five different networks and for five regions of ~~1000 GDD was reached~~Switzerland. ~~Light grey areas denote values where no climatology of a 1000 GDD threshold was calculated because the threshold was reached in less than 75% of the years between 1763~~ f) Autocorrelation at lag day 1 to ~~1812. Dark grey denotes areas where~~ 20 for the ~~threshold of 1000 GDD was not reached in~~ original grid and for five regions covering Switzerland. The analysis is performed on the ~~year 1816. c) Anomaly of number of cold days (days below the 20th percentile of daily mean temperature)~~ cross-validation results for ~~April~~ the period 1961 to ~~September 1816. d) Wet-days anomaly in percentage~~ 2020. See Fig. 1 for ~~April to September 1816. For comparison to~~ the ~~summer 1770, all anomalies are calculated with respect~~ network set-ups. The regions correspond to the ~~1763 to 1812 climatology, which does not include~~ major regions used for the ~~year 1816. Note, that the color scales are different from Fig~~national climate scenarios (?).~~10.~~
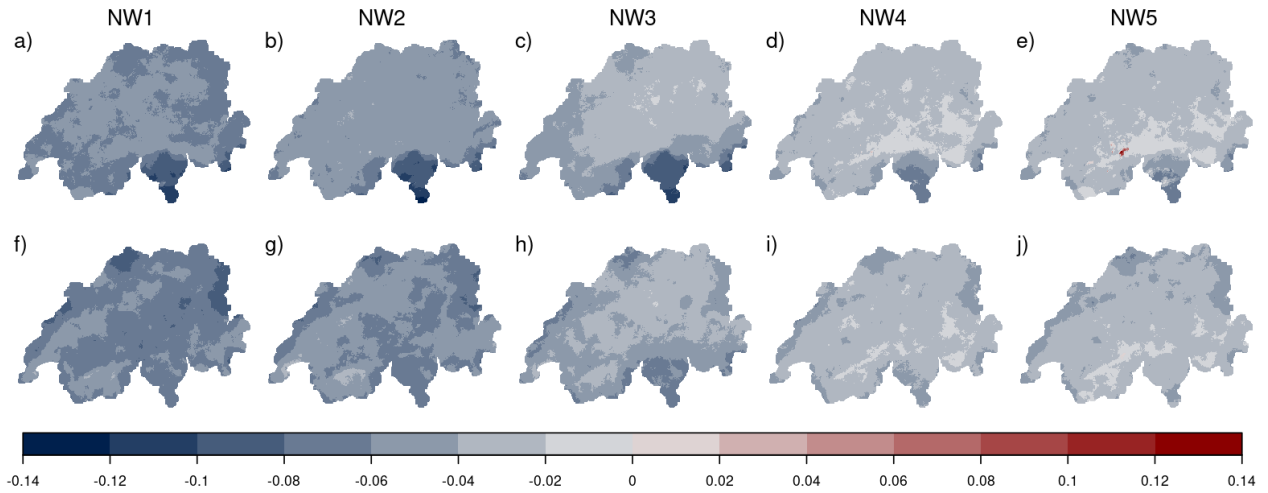
Figure A4. a-e) Differences in the fraction of wet days followed by wet days for the cross-validations of the five networks (see Fig. 1) compared to the original data set (cross-validation minus original). f-j) Same, but for the fraction of dry days followed by dry days. A wet day is defined as a day above 0.1 mm. The fractions are calculated across the entire cross-validation period 1961 to 2020.
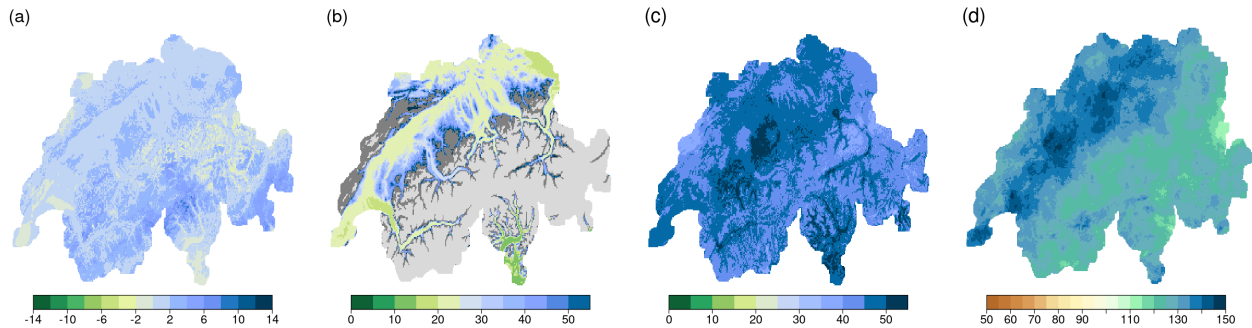
Figure A5. a) Anomaly of number of days with snowfall for April 1816. b) Anomaly in days for the year 1816 when the threshold of 1000 GDD was reached. Light grey areas denote values where no climatology of a 1000 GDD threshold was calculated because the threshold was reached in less than 75% of the years between 1763 to 1812. Dark grey denotes areas where the threshold of 1000 GDD was not reached in the year 1816. c) Anomaly of number of cold days (days below the 20th percentile of daily mean temperature) for April to September 1816. d) Wet-days anomaly in percentage for April to September 1816. For comparison to the summer 1770, all anomalies are calculated with respect to the 1763 to 1812 climatology, which does not include the year 1816. Note, that the color scales are different from Fig. 10.

595

Author contributions. NI performed the reconstruction and the case studies and wrote the manuscript. LP created the first version of the data set for the period 1864 to 2017. YB provided the historical observations. SB provided the idea for reconstruction and supervised the process. LP, YB, and SB contributed to the manuscript.

Competing interests. The authors declare that they have no conflict of interest.

References

Baertschi, A.: Wetterberichte einer Oberländischen Gemeinde vom 15.-19. Jahrhundert, in: Hardermannli. Illlustrierte Sonntagsbeilage zum Oberländer Volksblatt, 16, 1916.

Begert, M., Schlegel, T., and Kirchhofer, W.: Homogeneous temperature and precipitation series of Switzerland from 1864 to 2000, International Journal of Climatology, 25, 65–80, https://doi.org/10.1002/joc.1118, 2005.

Begert, M., Seiz, G., Foppa, N., Schlegel, T., Appenzeller, C., and Müller, G.: Die Überführung der klimatologischen Referenzstationen der Schweiz in das Swiss National Basic Climatological Network (Swiss NBCN), Arbeitsberichte der MeteoSchweiz, 215, 2007.

Bhend, J., Franke, J., Folini, D., Wild, M., and Brönnimann, S.: An ensemble-based approach to climate reconstructions, Climate of the Past, 8, 963–976, https://doi.org/10.5194/cp-8-963-2012, 2012.

Böhm, R., Jones, P. D., Hiebl, J., Frank, D., Brunetti, M., and Maugeri, M.: The early instrumental warm-bias: a solution for long central European temperature series 1760–2007, Climatic Change, 101, 41–67, https://doi.org/10.1007/s10584-009-9649-4, 2010.

Bonhomme, R.: Bases and limits to using 'degree. day'units, European Journal of Agronomy, 13, 1–10, 2000.

Brönnimann, S., ed.: Swiss Early Instrumental Meteorological Series, Geographica Bernensia G96, Bern, 2020.

Brönnimann, S.: From climate to weather reconstructions, PLOS Climate, 1, e0000 034, https://doi.org/10.1371/journal.pclm.0000034, 2022.

Brönnimann, S. and Brugnara, Y.: D'Annone's Meteorological Series from Basel, 1755–1804. Swiss Early Instrumental Meteorological Series, Bern: Geographica Bernensia, G96, 119–126, 2020a.

Brönnimann, S. and Brugnara, Y.: The meteorological series from the Great St. Bernard, 1817-1863. Swiss Early Instrumental Meteorological Series, Bern: Geographica Bernensia, G96, 109–117, 2020b.

Brönnimann, S. and Brugnara, Y.: Meteorological Series from Basel, 1825–1863. Swiss Early Instrumental Meteorological Series, Bern: Geographica Bernensia, G96, 127–138, 2021.

Brönnimann, S. and Brugnara, Y.: Nineteenth century meteorological records from Vevey, Einsiedeln,Bellinzona, Lucerne, Fribourg, and Zug. Swiss Early Instrumental Meteorological Series, Bern: Geographica Bernensia, G96, 245–259, 2022.

Brönnimann, S., Bühler, M., and Brugnara, Y.: The series from Geneva, 1799–1863. Swiss Early Instrumental Meteorological Series, Bern: Geographica Bernensia, G96, 47–59, 2020.

Brugnara, Y.: Early Instrumental Temperature Records for Basel, Bern, Geneva, and Zurich, https://doi.org/10.48620/74, 2022.

Brugnara, Y., Brönnimann, S., Zamuriano Carbajal, J. M., Schild, J., Rohr, C., and Segesser, D.: Reanalysis sheds lights on 1916 avalanche disaster, ECMWF Newsletter, pp. 28–34, https://doi.org/10.21957/h9b197, 2017.

Brugnara, Y., Gilabert, A., Ventura, C., and Hunziker, S.: dataresqc: Quality control tools for climate data developed by the C3S Data Rescue Service, 2019.

Brugnara, Y., Flückiger, J., and Brönnimann, S.: Instruments, procedures, processing, and analyses. Swiss Early Instrumental Meteorological Series., Bern: Geographica Bernensia, G96, 17–32, 2020a.

Brugnara, Y., Pfister, L., Villiger, L., Rohr, C., Isotta, F. A., and Brönnimann, S.: Early instrumental meteorological observations in Switzerland: 1708–1873, Earth System Science Data, 12, 1179–1190, https://doi.org/10.5194/essd-12-1179-2020, 2020b.

Brugnara, Y., Hari, C., Pfister, L., Valler, V., and Brönnimann, S.: Pre-industrial Temperature Variability on the Swiss Plateau Derived from the Instrumental Daily Series of Bern and Zurich, Climate of the Past Discussions, pp. 1–34, https://doi.org/10.5194/cp-2022-34, 2022.

Brönnimann, S., Allan, R., Ashcroft, L., Baer, S., Barriendos, M., Brázdil, R., Brugnara, Y., Brunet, M., Brunetti, M., Chimani, B., Cornes, R., Domínguez-Castro, F., Filipiak, J., Founda, D., Herrera, R. G., Gergis, J., Grab, S., Hannak, L., Huhtamaa, H., Jacobsen, K. S., Jones,

P., Jourdain, S., Kiss, A., Lin, K. E., Lorrey, A., Lundstad, E., Luterbacher, J., Mauelshagen, F., Maugeri, M., Maughan, N., Moberg, A., Neukom, R., Nicholson, S., Noone, S., Øyvind Nordli, Ólafsdóttir, K. B., Pearce, P. R., Pfister, L., Pribyl, K., Przybylak, R., Pudmenzky, C., Rasol, D., Reichenbach, D., Řezníčková, L., Rodrigo, F. S., Rohr, C., Skrynyk, O., Slonosky, V., Thorne, P., Valente, M. A., Vaquero, J. M., Westcott, N. E., Williamson, F., and Wyszyński", P.: Unlocking Pre-1850 Instrumental Meteorological Records: A Global Inventory, Bulletin of the American Meteorological Society, 100, ES389 – ES413, https://doi.org/10.1175/BAMS-D-19-0040.1, 2019.

Caillouet, L., Vidal, J.-P., Sauquet, E., Graff, B., and Soubeyroux, J.-M.: SCOPE Climate: a 142-year daily high-resolution ensemble meteorological reconstruction dataset over France, Earth System Science Data, 11, 241–260, https://doi.org/10.5194/essd-11-241-2019, 2019.

Camuffo, D. and Jones, P.: Improved understanding of past climatic variability from early daily European instrumental sources, Springer Dordrecht, https://doi.org/10.1007/978-94-010-0371-1, 2002.

Casty, C., Wanner, H., Luterbacher, J., Esper, J., and Böhm, R.: Temperature and precipitation variability in the European Alps since 1500, International Journal of Climatology, 25, 1855–1880, https://doi.org/10.1002/joc.1216, 2005.

Casty, C., Raible, C. C., Stocker, T. F., Wanner, H., and Luterbacher, J.: A European pattern climatology 1766–2000, Climate Dynamics, 29, 791–805, https://doi.org/10.1007/s00382-007-0257-6, 2007.

Collet, D.: Die doppelte Katastrophe: Klima und Kultur in der europäischen Hungerkrise 1770–1772., vol. 18 of *Umwelt und Gesellschaft*, Vandenhoeck & Ruprecht, https://doi.org/10.13109/9783666355929, 2018.

Cook, E. R., Seager, R., Kushnir, Y., Briffa, K. R., Büntgen, U., Frank, D., Krusic, P. J., Tegel, W., van der Schrier, G., Andreu-Hayles, L., et al.: Old World megadroughts and pluvials during the Common Era, Science Advances, 1, e1500 561, 2015.

Cornes, R. C., van der Schrier, G., van den Besselaar, E. J., and Jones, P. D.: An ensemble version of the E-OBS temperature and precipitation data sets, Journal of Geophysical Research: Atmospheres, 123, 9391–9409, https://doi.org/10.1029/2017JD028200, 2018.

Devers, A., Vidal, J.-P., Lauvernet, C., and Vannier, O.: FYRE Climate: a high-resolution reanalysis of daily precipitation and temperature in France from 1871 to 2012, Climate of the Past, 17, 1857–1879, https://doi.org/10.5194/cp-17-1857-2021, 2021.

Dobrovolnỳ, P., Moberg, A., Brázdil, R., Pfister, C., Glaser, R., Wilson, R., van Engelen, A., Limanówka, D., Kiss, A., Halíčková, M., et al.: Monthly, seasonal and annual temperature reconstructions for Central Europe derived from documentary evidence and instrumental records since AD 1500, Climatic Change, 101, 69–107, https://doi.org/10.1007/s10584-009-9724-x, 2010.

Estévez, J., Gavilán, P., and García-Marín, A.: Spatial regression test for ensuring temperature data quality in southern Spain, Theoretical and Applied Climatology, 131, 309–318, https://doi.org/10.1007/s00704-016-1982-8, 2018.

Faden, M., Villiger, L., Brugnara, Y., and Brönnimann, S.: The meteorological series from Aarau, 1807–1865. Swiss Early Instrumental Meteorological Series, Bern: Geographica Bernensia, G96, 61–72, 2020.

Feigenwinter, I., Kotlarski, S., Casanueva, A., Schwierz, C., and Liniger, M.: Exploring quantile mapping as a tool to produce user-tailored climate scenarios for Switzerland, MeteoSchweiz, 2018.

Flückiger, S., Brönnimann, S., Holzkämper, A., Fuhrer, J., Krämer, D., Pfister, C., and Rohr, C.: Simulating crop yield losses in Switzerland for historical and present Tambora climate scenarios, Environmental Research Letters, 12, 074 026, https://doi.org/10.1088/1748-9326/aa7246, 2017.

Franke, J., Brönnimann, S., Bhend, J., and Brugnara, Y.: A monthly global paleo-reanalysis of the atmosphere from 1600 to 2005 for studying past climatic variations, Scientific Data, 4, 1–19, https://doi.org/10.1038/sdata.2017.76, 2017.

Frei, C.: Interpolation of temperature in a mountainous region using nonlinear profiles and non-Euclidean distances, International Journal of Climatology, 34, 1585–1605, https://doi.org/10.1002/joc.3786, 2014.

Füllemann, C., Begert, M., Croci-Maspoli, M., and Bönnimann, S.: Digitalisieren und Homogenisieren von historischen Klimadaten des Swiss NBCN: Resultate aus DigiHom, Arbeitsberichte der MeteoSchweiz, 236, 2011.

680 Gómez-Navarro, J. J., Zorita, E., Raible, C. C., and Neukom, R.: Pseudo-proxy tests of the analogue method to reconstruct spatially resolved global temperature during the Common Era, Climate of the Past, 13, 629–648, https://doi.org/10.5194/cp-13-629-2017, 2017.

Gower, J. C.: A general coefficient of similarity and some of its properties, Biometrics, pp. 857–871, https://doi.org/10.2307/2528823, 1971.

Gudmundsson, L., Bremnes, J. B., Haugen, J. E., and Engen-Skaugen, T.: Downscaling RCM precipitation to the station scale using statistical transformations–a comparison of methods, Hydrology and Earth System Sciences, 16, 3383–3390, https://doi.org/10.5194/hessd-9-6185-
685 2012, 2012.

Häderli, S., Pfister, S. M., Villiger, L., Brugnara, Y., and Brönnimann, S.: Two meteorological series from Geneva, 1782–1791. Swiss Early Instrumental Meteorological Series, Bern: Geographica Bernensia, G96, 33–46, 2020.

Hari, C., Brugnara, Y., Rohr, C., and Brönnimann, S.: Meteorological Observations in Bern and Vicinity, 1777-1834. Swiss Early Instrumental Meteorological Series, Bern: Geographica Bernensia, G96, 199–211, 2022.

690 Harvey-Fishenden, A. and Macdonald, N.: Evaluating the utility of qualitative personal diaries in precipitation reconstruction in the eighteenth and nineteenth centuries, Climate of the Past, 17, 133–149, https://doi.org/10.5194/cp-17-133-2021, 2021.

Hersbach, H., Bell, B., Berrisford, P., Hirahara, S., Horányi, A., Muñoz-Sabater, J., Nicolas, J., Peubey, C., Radu, R., Schepers, D., et al.: The ERA5 global reanalysis, Quarterly Journal of the Royal Meteorological Society, 146, 1999–2049, https://doi.org/10.1002/qj.3803, 2020.

Hupfer, F.: Das Wetter der Nation: Meteorologie, Klimatologie und der schweizerische Bundesstaat, 1860–1914, Chronos Verlag, 2019.

695 Hürzeler, A., Brugnara, Y., and Brönnimann, S.: The meteorological record from St. Gall, 1812–1853. Swiss Early Instrumental Meteorological Series, Bern: Geographica Bernensia, G96, 87–95, 2020.

Imfeld, N.: Daily high-resolution temperature and precipitation fields for Switzerland from 1763 to 2020, http://giub-torrent.unibe.ch/swiss_reconstruction/, 2022.

Isotta, F. A., Begert, M., and Frei, C.: Long-term consistent monthly temperature and precipitation grid data sets for Switzerland over the
700 past 150 years, Journal of Geophysical Research: Atmospheres, 124, 3783–3799, https://doi.org/10.1029/2018JD029910, 2019.

Jennings, K. S., Winchell, T. S., Livneh, B., and Molotch, N. P.: Spatial variation of the rain–snow temperature threshold across the Northern Hemisphere, Nature communications, 9, 1–9, https://doi.org/10.1038/s41467-018-03629-7, 2018.

Keller, V., Tanguy, M., Prosdocimi, I., Terry, J., Hitt, O., Cole, S., Fry, M., Morris, D., and Dixon, H.: CEH-GEAR: 1 km resolution daily and monthly areal rainfall estimates for the UK for hydrological and other applications, Earth System Science Data, 7, 143–155,
705 https://doi.org/10.5194/essd-7-143-2015, 2015.

Kienzle, S. W.: A new temperature based method to separate rain and snow, Hydrological Processes, 22, 5067–5085, https://doi.org/10.1002/hyp.7131, 2008.

Klein Tank, A., Wijngaard, J., Können, G., Böhm, R., Demarée, G., Gocheva, A., Mileta, M., Pashiardis, S., Hejkrlik, L., Kern-Hansen, C., et al.: Daily dataset of 20th-century surface air temperature and precipitation series for the European Climate Assessment, International
710 Journal of Climatology, 22, 1441–1453, https://doi.org/10.1002/joc.773, 2002.

Kohler, X.: Observations Météorologiques, Économiques et Rurales dans l'Erguel et la Prévôté de Moutier de 1747 à 1804 par le pasteur T. Frêne, in: Actes de la Société Jurassienne d' Émulation, 22, pp. 213–267, 1871.

Kuhn, M. and Johnson, K.: Feature engineering and selection: A practical approach for predictive models, CRC Press, 2019.

Luterbacher, J. and Pfister, C.: The year without a summer, Nature Geoscience, 8, 246–248, https://doi.org/10.1038/ngeo2404, 2015.

Luterbacher, J., Dietrich, D., Xoplaki, E., Grosjean, M., and Wanner, H.: European Seasonal and Annual Temperature Variability, Trends, and Extremes Since 1500, Science, 303, 1499–1503, https://doi.org/10.1126/science.1093877, 2004.

MeteoSwiss: Documentation of MeteoSwiss Grid-Data Products. Daily Precipitation (final analysis): RhiresD, https://www.meteoswiss.admin.ch/content/dam/meteoswiss/de/service-und-publikationen/produkt/raeumliche-daten-niederschlag/doc/ProdDoc_RhiresD.pdf, [Online; accessed 30-June-2022], 2021a.

MeteoSwiss: Documentation of MeteoSwiss Grid-Data Products. Daily Mean, Minimum and Maximum Temperature: TabsD, TminD, TmaxD, https://www.meteoswiss.admin.ch/content/dam/meteoswiss/de/service-und-publikationen/produkt/raeumliche-daten-temperatur/doc/ProdDoc_TabsD.pdf, [Online; accessed 30-June-2022], 2021b.

MeteoSwiss: Documentation of MeteoSwiss Grid-Data Products. Monthly Temperature and Precipitation Reconstructions, https://www.meteoschweiz.admin.ch/dam/jcr:98a965e5-30dd-4fdf-a42b-74c414a4a731/ProdDoc_rec.pdf, [Online; accessed 07-February-2023], 2021c.

Miller, P., Lanier, W., and Brandt, S.: Using growing degree days to predict plant stages, Montguide MT200103 AG, 2001.

Moon, H., Gudmundsson, L., Guillod, B. P., Venugopal, V., and Seneviratne, S. I.: Intercomparison of daily precipitation persistence in multiple global observations and climate models, Environmental Research Letters, 14, 105 009, 2019.

Muñoz-Sabater, J., Dutra, E., Agustí-Panareda, A., Albergel, C., Arduini, G., Balsamo, G., Boussetta, S., Choulga, M., Harrigan, S., Hersbach, H., et al.: ERA5-Land: A state-of-the-art global reanalysis dataset for land applications, Earth System Science Data, 13, 4349–4383, https://doi.org/10.5194/essd-13-4349-2021, 2021.

Murphy, C., Wilby, R. L., Matthews, T., Horvath, C., Crampsie, A., Ludlow, F., Noone, S., Brannigan, J., Hannaford, J., McLeman, R., et al.: The forgotten drought of 1765–1768: Reconstructing and re-evaluating historical droughts in the British and Irish Isles, International Journal of Climatology, 40, 5329–5351, https://doi.org/10.1002/joc.6521, 2020.

Paffrath, J.: Schriften des Vereins für die Geschichte des Bodensees und seiner Umgebung, chap. Zum Wetterverlauf am Bodensee, Kommissionsverlag von Joh. Thom. Stettner, Lindau, 1915.

PAGES2kConsortium: Continental-scale temperature variability during the past two millennia, Nature Geoscience, 6, 339–346, https://doi.org/10.1038/ngeo1797, 2013.

Pappert, D., Barriendos, M., Brugnara, Y., Imfeld, N., Jourdain, S., Przybylak, R., Rohr, C., and Brönnimann, S.: Statistical reconstruction of daily temperature and sea-level pressure in Europe for the severe winter 1788/9, Climate of the Past Discussions, pp. 1–35, 2022.

Pauling, A., Luterbacher, J., Casty, C., and Wanner, H.: Five hundred years of gridded high-resolution precipitation reconstructions over Europe and the connection to large-scale circulation, Climate Dynamics, 26, 387–405, https://doi.org/10.1007/s00382-005-0090-8, 2006.

Pfister, C.: Agrarkonjunktur und Witterungsverlauf im westlichen schweizer Mittelland zur Zeit der ökonomischen Patrioten, 1755-1797: ein Beitrag zur Umwelt-u. Wirtschaftsgeschichte des 18. Jahrhunderts, vol. 2, Lang Druck AG, 1975.

Pfister, C.: Das Klima der Schweiz von 1525-1860 und seine Bedeutung in der Geschichte von Bevölkerung und Landwirtschaft, vol. 1, Haupt, 1988.

Pfister, C. and Brázdil, R.: Social vulnerability to climate in the" Little Ice Age": an example from Central Europe in the early 1770s, Climate of the Past, 2, 115–129, https://doi.org/10.5194/cp-2-115-2006, 2006.

Pfister, C. and Wanner, H.: Klima und Gesellschaft in Europa. Die letzten tausend Jahre, Haupt Verlag, 2021.

Pfister, C., Rohr, C., and Jover, A. C. C.: Euro-Climhist: eine Datenplattform der Universität Bern zur Witterungs-, Klima-und Katastrophengeschichte, Wasser Energie Luft, 109, https://doi.org/10.7892/boris.97013, 2017.

Pfister, L., Hupfer, F., Brugnara, Y., Munz, L., Villiger, L., Meyer, L., Schwander, M., Isotta, F. A., Rohr, C., and Brönnimann, S.: Early instrumental meteorological measurements in Switzerland, Climate of the Past, 15, 1345–1361, https://doi.org/10.5194/cp-15-1345-2019, 2019.

755 Pfister, L., Brönnimann, S., Schwander, M., Isotta, F. A., Horton, P., and Rohr, C.: Statistical reconstruction of daily precipitation and temperature fields in Switzerland back to 1864, Climate of the Past, 16, 663–678, https://doi.org/10.5194/cp-16-663-2020, 2020.

Piuz, A.-M.: Climat, récoltes et vie des hommes à Genève, XVIe-XVIIIe siècle, Annales. Histoire, Sciences Sociales, 29, 599–618, https://doi.org/10.3406/ahess.1974.293496, 1974.

Rajczak, J., Kotlarski, S., and Schär, C.: Does quantile mapping of simulated precipitation correct for biases in transition probabilities and 760 spell lengths?, Journal of Climate, 29, 1605–1615, https://doi.org/10.1175/JCLI-D-15-0162.1, 2016.

Rössler, O. and Brönnimann, S.: The effect of the Tambora eruption on Swiss flood generation in 1816/1817, Science of The Total Environment, 627, 1218–1227, https://doi.org/10.1016/j.scitotenv.2018.01.254, 2018.

Rutishauser, T., Brönnimann, S., Gehrig, R., Pietragalla, B., Baumgarten, F., Vitasse, Y., Stöckli, S., Pfister, C., Holzkämper, A., Hund, A., Fossati, D., Meier, M., Weingartner, R., and Buchmann, M.: Klimawandel und Jahreszeiten (Reihe G Grundlagenforschung G97), 765 Geographica Bernensia, 2020.

Schaller-Donauer, A.: Chronik der Naturereignisse im Urnerland 1000-1800, Gotthardpost, 1937.

Schenk, F. and Zorita, E.: Reconstruction of high resolution atmospheric fields for Northern Europe using analog-upscaling, Climate of the Past, 8, 1681–1703, https://doi.org/10.5194/cp-8-1681-2012, 2012.

Scherrer, S. C. and Appenzeller, C.: Fog and low stratus over the Swiss Plateau- a climatological study, International Journal of Climatology, 770 34, 678–686, https://doi.org/10.1002/joc.3714, 2014.

Schwander, M., Brönnimann, S., Delaygue, G., Rohrer, M., Auchmann, R., and Brugnara, Y.: Reconstruction of Central European daily weather types back to 1763, International Journal of Climatology, 37, 30–44, https://doi.org/10.1002/joc.4974, 2017.

Slivinski, L. C., Compo, G. P., Whitaker, J. S., Sardeshmukh, P. D., Giese, B. S., McColl, C., Allan, R., Yin, X., Vose, R., Titchner, H., et al.: Towards a more reliable historical reanalysis: Improvements for version 3 of the Twentieth Century Reanalysis system, Quarterly Journal 775 of the Royal Meteorological Society, 145, 2876–2908, https://doi.org/10.1002/qj.3598, 2019.

Strasser, G.: Grindelwaldner Chroniken, Gletschermann. Familienblatt für Grindelwald, 1890.

Stucki, P., Brönnimann, S., Martius, O., Welker, C., Rickli, R., Dierer, S., Bresch, D. N., Compo, G. P., and Sardeshmukh, P. D.: Dynamical downscaling and loss modeling for the reconstruction of historical weather extremes and their impacts: a severe Foehn storm in 1925, Bulletin of the American Meteorological Society, 96, 1233–1241, https://doi.org/10.1175/BAMS-D-14-00041.1, 2015.

780 Trümpi, C.: Neuere Glarner Chronik, Verlag Heinrich Steiners und Comp. und der Herren Buchbinder, 1774.

Valler, V., Franke, J., Brugnara, Y., and Brönnimann, S.: An updated global atmospheric paleo-reanalysis covering the last 400 years, Geoscience Data Journal, p. 89–107, https://doi.org/10.1002/gdj3.121, 2022.

Walser, G.: Neue Appenzeller Chronik oder Geschichte des Landes Appenzell der Innern und Aussern Rhoden, vol. 1-2, https://doi.org/10.3931/e-rara-24883, 1731.

785 Wang, X., Toride, K., and Yoshimura, K.: Impact of Gaussian Transformation on Cloud Cover Data Assimilation for Historical Weather Reconstruction, Earth and Space Science Open Archive ESSOAr, https://doi.org/10.1002/essoar.10506932.2, 2021.

Wang, X. L.: Penalized maximal F test for detecting undocumented mean shift without trend change, Journal of Atmospheric and Oceanic Technology, 25, 368–384, https://doi.org/10.1175/2007JTECHA982.1, 2008.

Wang, X. L. and Feng, Y.: RHtestsV4 user manual, Climate Research Division, Atmospheric Science and Technology Directorate, Science and Technology Branch, Environment Canada, 28, 2013.

Wang, X. L., Wen, Q. H., and Wu, Y.: Penalized maximal t test for detecting undocumented mean change in climate data series, Journal of Applied Meteorology and Climatology, 46, 916–931, https://doi.org/10.1175/JAM2504.1, 2007.

Wartenburger, R., Brönnimann, S., and Stickler, A.: Observation errors in early historical upper-air observations, Journal of Geophysical Research: Atmospheres, 118, 12–012, https://doi.org/10.1002/2013JD020156, 2013.

Weber, J., Brugnara, Y., and Brönnimann, S.: Two meteorological series from Herisau, 1821–1844. Swiss Early Instrumental Meteorological Series, Bern: Geographica Bernensia, G96, 73–85, 2020.

Weusthoff, T.: Weather Type Classification at MeteoSwiss-Introduction of new automatic classification schemes. Arbeitsberichte der MeteoSchweiz, 235, 46, 2011.

Whitaker, J. S. and Hamill, T. M.: Ensemble data assimilation without perturbed observations, Monthly Weather Review, 130, 1913–1924, https://doi.org/10.1175/1520-0493(2002)130%3C1913:EDAWPO%3E2.0.CO;2, 2002.

Wilks, D. S.: Statistical methods in the atmospheric sciences, vol. 100, Academic press, 2011.

Winkler, P.: Hohenpeißenberg: 1781-2006; das älteste Bergobservatorium der Welt; 225 Jahre Meteorologisches Observatorium Hohenpeißenberg, Deutscher Wetterdienst, 2006.

Wyer, V., Brugnara, Y., and Brönnimann, S.: Meteorological Series from Neuchâtel, Bern, and Gurzelen from the 18th Century. Swiss Early Instrumental Meteorological Series, Bern: Geographica Bernensia, G96, 169–182, 2021.

Wypych, A., Sulikowska, A., Ustrnul, Z., and Czekierda, D.: Variability of growing degree days in Poland in response to ongoing climate changes in Europe, International Journal of Biometeorology, 61, 49–59, https://doi.org/10.1007/s00484-016-1190-3, 2017.

Zubler, E. M., Scherrer, S. C., Croci-Maspoli, M., Liniger, M. A., and Appenzeller, C.: Key climate indices in Switzerland; expected changes in a future climate, Climatic change, 123, 255–271, 2014.

Zumbühl, H. J.: Die Schwankungen des Unteren Grindelwaldgletschers, in: Die Schwankungen der Grindelwaldgletscher in den historischen Bild-und Schriftquellen des 12. bis 19. Jahrhunderts, pp. 15–55, Springer, 1980.